haematologica
Journal of the Ferrata Storti Foundation

Hematopoiesis post anti-CD117 monoclonal antibody treatment in wild-type and Fanconi anemia settings

by Morgane Denis, Leah Swartzrock, Hana Willner, Quenton R. Bubb, Ethan Haslett, Yan Yi Chan, Anzhi Chen, Mark R. Krampf, and Agnieszka D. Czechowicz

Received: October 5, 2023.
Accepted: March 26, 2024.

Citation: Morgane Denis, Leah Swartzrock, Hana Willner, Quenton R. Bubb, Ethan Haslett, Yan Yi Chan, Anzhi Chen, Mark R. Krampf, and Agnieszka D. Czechowicz. Hematopoiesis post anti-CD117 monoclonal antibody treatment in wild-type and Fanconi anemia settings.
Haematologica. 2024 Apr 4. doi: 10.3324/haematol.2023.284275 [Epub ahead of print]

Hematopoiesis post anti-CD117 monoclonal antibody treatment in wild-type and Fanconi anemia settings

Authors

Morgane Denis[1,2,3], Leah Swartzrock[1,2,3], Hana Willner[1,2,3], Quenton R. Bubb[1,2,3], Ethan Haslett[1,2,3], Yan Yi Chan[1,2,3], Anzhi Chen[1,2,3], Mark R. Krampf[1,2,3] and Agnieszka D. Czechowicz[1,2,3]

Affiliations

[1]Division of Hematology, Oncology, Stem Cell Transplantation and Regenerative Medicine, Department of Pediatrics, Stanford University School of Medicine, Stanford, California.

[2]Institute for Stem Cell Biology and Regenerative Medicine, Stanford University School of Medicine, Stanford, California.

[3]Center for Definitive and Curative Medicine, Stanford University School of Medicine, Stanford, California.

Authors' contributions

M.D., Y.Y.C., A.Ch. and A.D.C. designed the study; M.D., L.S., H.W., E.H., Y.Y.C., A.Ch., and M.R.K. performed research and analyzed data; L.S. and E.H. managed animal colonies and provided technical assistance; M.D., Q.R.B. and A.D.C. interpreted data; and M.D. and A.D.C. wrote the manuscript. A.D.C. provided mentorship to the first author.

Running heads: Impact of anti-CD117 antibody treatment on hematopoiesis

Article Summary: In this study, we examined the short-term and long-term effects of antagonistic anti-CD117 mAb treatment in mice, focusing on its safety and potential impact on hematopoietic stem cells (HSCs) in the context of wild-type (WT) and Fanconi Anemia (FA) settings. We conducted various assessments including DNA damage assays, flow cytometry analysis of HSC and progenitor populations, and single-cell RNA sequencing, revealing that one-time antagonistic anti-CD117 mAb treatment induced only transient effects, demonstrating the safety of this approach and potential clinical utility as a conditioning agent for hematopoietic stem cell transplantation. Further, these results highlight the comprehensive impact of antagonistic anti-CD117 mAbs on hematopoiesis in both WT and FA settings.

Corresponding author

Agnieszka D. Czechowicz: aneeshka@stanford.edu

Data-sharing statement

Data that support the findings of this study are available from the corresponding author upon reasonable request.

Acknowledgments

The authors thank Dr. Kenneth I. Weinberg, Stanford University for his generous gift of the Fancd2$^{-/-}$ mice, which originated from Dr. Marcus Grompe at Oregon Health and Science University. They also thank Amelia Scheck and Cynthia Klein, Stanford University for their help with laboratory management. Moreover, the authors thank the Stanford Stem Cell Institute FACS Core for flow cytometry access, and the Stanford Functional Genomics Facility for performing single cell RNA sequencing. Figures were created with BioRender.

Funding

This project was funded by a grant to A.D.C. from the Fanconi Anemia Research Fund and United States Department of Defense (W81XWH2110262).

This manuscript contains 4 figures with 2 supplementary files (one PDF file and one Excel table).

Disclosures

A.D.C. discloses financial interests in the following entities working in the rare genetic disease space: Beam Therapeutics, Decibel Therapeutics, Editas Medicines, GV, Magenta Therapeutics, Prime Medicines and Spotlight Therapeutics.

Abstract

Anti-CD117 monoclonal antibody (mAb) agents have emerged as exciting alternative conditioning strategies to traditional genotoxic irradiation or chemotherapy conditioning for both allogeneic and autologous gene-modified hematopoietic stem cell transplantation. Further, these agents are concurrently being explored in the treatment of mast cell disorders. Despite promising results in animal models and more recently in patients, the short-term and long-term effects of these treatments have not been fully explored. We conducted rigorous assessments to evaluate the effects of antagonistic anti-mCD117 mAb, ACK2, on hematopoiesis in wild-type (WT) and Fanconi Anemia (FA) mice. Importantly, we found no evidence of short-term DNA damage in either setting following this treatment suggesting that ACK2 does not induce immediate genotoxicity, providing crucial insights into its safety profile. Surprisingly, FA mice exhibited an increase in colony formation post-ACK2 treatment without accompanying DNA damage, indicating a potential targeting of hematopoietic stem cells (HSCs) and expansion of hematopoietic progenitor cells. Moreover, the long-term phenotypic and functional changes in hematopoietic stem and progenitor cells did not significantly differ between the ACK2-treated and control groups, in either setting, supporting that ACK2 does not adversely affect hematopoietic capacity. These finding underscore the safety of these agents when utilized as a short-course treatment in the conditioning context, as they did not induce significant changes in DNA damage amongst hematopoietic stem or progenitor cells. However, through a comparison of gene expression via single-cell RNA sequencing between untreated and treated mice, it was revealed that the ACK2 mAb, via c-Kit downregulation, effectively modulated the MAPK pathway with Fos down-regulation in WT and FA mice. Importantly, this modulation was achieved without causing prolonged disruptions. These findings validate the safety of the treatment and also enhance our understanding of its intricate mode of action at the molecular level.

Introduction

Bone marrow transplantation/hematopoietic stem cell transplantation (BMT/HSCT) is a powerful curative treatment for many different blood and immune diseases – including both non-malignant and malignant diseases that affects millions of people world-wide. Further, it is the only proven therapy for Bone Marrow Failure (BMF) syndromes such as Fanconi Anemia (FA)[1]. While BMF can arise from a variety of genetic or acquired factors, in both scenarios, hematopoietic stem cells (HSCs) and hematopoietic progenitor are lost leading to a decline of blood and immune cell production which leads to anemia, thrombocytopenia, and neutropenia. Only through replacement of HSCs from a healthy donor can definitive cure be achieved. FA is one of the most frequent genetic causes of BMF, arising from mutations in the Fanconi anemia complementation (FANC) genes, which are required for repairing DNA interstrand crosslinks (ICL)[2]. FA patients have chromosomal fragility leading to hematopoietic failure (aplastic anemia, myelodysplasia, or leukemia), increased systemic cancer susceptibility, other rare organ dysfunction such as congenital structural anomalies[3,4] and ultimately shortened lifespans. Given that >90% of FA patients develop hematopoietic failure over their lifetimes, almost all require HSCT[5].

While HSCT can effectively replace a defective blood and immune system, current transplantation methods necessitate the use of nonspecific, genotoxic chemotherapy and/or irradiation conditioning[6]. These conventional conditioning methods cause substantial DNA damage that is typically repaired by DNA repair pathways that necessitate the FA proteins. Consequently, the resulting multi-organ damage, mucositis, infertility, and secondary malignancies from classic conditioning are especially profound in FA patients who are unable to repair ICL[1]. This leads to considerable morbidity and mortality in this particularly vulnerable patient group, and restricts use of BMT/HSCT primarily to patients with severe hematopoietic failure or malignant transformation[7,8]. To improve outcomes for all individuals requiring HSCT, including those with FA, it is crucial to identify a safe, non-genotoxic conditioning strategy.

Over the past decade, various alternative antibody-based conditioning strategies have been developed by our group and others to improve the safety and efficacy of BMT/HSCT. Based upon experiments showcasing that competing HSCs limited engraftment[8], our group initially pioneered a novel antibody-based conditioning approach by targeting the HSC surface protein, c-

Kit (CD117), using antagonistic anti-mouse(m)CD117 monoclonal antibodies (mAbs) which we found caused effective depletion of host HSCs in certain mouse models, enabling non-toxic BMT/HSCT[9,10]. Given these results, clinical equivalent antagonistic anti-human(h)CD117 mAbs have been developed which have shown promise in human xenografts and in a recent pivotal clinical trial in patients with severe combined immunodeficiency (SCID)[11,12]. Moreover, these strategies could potentially improve outcomes for all types of genetic and acquired blood and immune diseases and thus are now being tested in a variety of clinical trials. These include as conditioning agents for HSCT for myelodysplastic syndrome/acute myeloid leukemia, hemoglobinopathies, and FA, as well as for treatment of mast cell disorders. However, an important question remains for the translation of these strategies to patients especially those with FA that are known to be more fragile, is if the antagonistic anti-CD117 mAbs induce cellular stresses and DNA damage on HSCs in the short-term or long-term.

The preliminary safety of antagonistic anti-CD117 mAbs has been established in wild-type (WT) mouse models, nonhuman primates, normal human xenografts and short-term in patients with SCID with no evidence of resulting myelodysplastic syndrome (MDS) or leukemia. However, a more substantive evaluation of cellular and genotoxic stresses in association with antagonistic anti-CD117 mAb treatments is needed to understand their effects, especially in DNA-repair defective genetic backgrounds such as FA. We have addressed this question by assessing changes in transcriptomic profiles of HSCs and progenitors by single-cell RNA sequencing (scRNA-seq) analysis as well as genotoxicity and systemic toxicity in response to anti-mCD117 mAb - ACK2 treatment in wild-type (WT) C57BL/6N mice, as well as FA complementation group D2 knockout ($FANCD2^{-/-}$) mice – which model the disease and display a hematopoietic phenotype. While prior studies have showcased the utility of antagonistic anti-CD117 mAbs in this and other FA mouse models[13,14], our study underscores the safety of this treatment in FA mice, both in the short and long term, with no evidence of DNA damage induction. Moreover, our investigation into potential downstream effects reveals intriguing disruptions various regulatory pathways including the MAPK pathway with downregulation of Fos, opening avenues for further exploration of antagonistic anti-mCD117 mAbs as therapeutic agents in the context of BMF and other conditions. These findings contribute valuable insights that may inform future clinical studies and therapeutic approaches for various hematological

disorders including FA. This work is especially timely as the parallel anti-hCD117 mAbs clinical agents are currently being tested in these settings.

Methods

Mice

All animal housing and procedures were approved by the institutional ethics Animal Care and Use Committee at Stanford University. FANCD2$^{-/-}$ mice were a generous gift from Dr. Kenneth I. Weinberg (Stanford University) which originated from Dr. Marcus Grompe at Oregon Health and Science University[15]. Mice were backcrossed onto C57BL/6N (CD45.2), originally derived on a 129/SvJ background. Designate WT C57BL/6N mice were purchased at Charles River Laboratories. In all studies, adult female and male animals, between 8 to 12 weeks of age were used.

Antibody treatment

200ug of Benadryl (Sigma-Aldrich, St Louis, MO) was given via intra-peritoneal injection, followed by anti-mCD117 ACK2 mAb (BioXcell) or IgG mAb (Sigma) which were administered intravenously as a one-time dose of 500μg per animal as previously published[10]. For each experiment, after 1 week or 24 weeks post treatment (Untreated, IgG and ACK2), blood was collected, and mice were euthanized to collect whole bone marrow (WBM) from tibia, femur, pelvis and spine. Cell suspensions from WBM were divided for each experiment described as follows.

Colony Formation Cell Assay

12,000 WBM cells were plated in triplicate in methylcellulose culture of Methocult (M3434, StemCell Technologies, Vancouver, Canada). Colony formation was evaluated 7 days post culture by StemVision (StemCell Technologies) and recorded accordingly.

Immunofluorescence yH2AX

After c-Kit enrichment on WBM using autoMACS® Columns (CD117 MicroBeads, mouse, 130-091-224, Miltenyi Biotec), 250,000 c-Kit enriched cells were resuspend in 100uL 1x PBS and pipetted directly onto poly-L-lysine coated coverslip. After fixing the cells with 3.7%

formaldehyde/PBS, cells were stained. Briefly, after permeabilization and 1 hour of blocking with 2% BSA/PBS 0.1% Tween 20, we stained with 1:250 yH2AX antibody (clone JBW301, Millipore) for 1 hour at room temperature. After washing cycle, the secondary antibody goat anti-Mouse IgG Alexa Fluor 488 was added at 1:1000 for 1 hour at room temperature. After the wash cycle the coverslip was mounted onto DAPI Fluoromount-G on a microscope slide. Scans of the slides were done with Keyence Microscopy and counts were performed with ImageJ software.

Micronuclei assay

Blood was collected via retro-orbital bleed with 2x heparinized capillary tubes into EDTA coated BD Microtainer® tubes. The assay was performed as previously described[16]. Briefly, the heparin red-blood cells were mixed directly over 2 ml cold methanol taken directly from -80 °C and stored at -80 °C for at least 12 hours. Staining was done with anti-CD71-FITC (Southern Biotech) and anti-CD61-BV421 (BD bioscience) in a solution containing 5 mg/mL RNase (Sigma) for 45 minutes at 4 °C with gentle agitation. After washing with bicarbonate buffer, cells were resuspended in bicarbonate buffer containing 5mg/mL PI and analyzed on FACSymphony A5 (BD Biosciences, San Jose, CA).

Flow cytometry

$1x10^6$ WBM cells were stained with the following antibodies for 30 minutes at 4°C in the dark. After washing with PBS 1X, cells were analyzed using a BD FACSymphony A5 (BD Biosciences, San Jose, CA). FlowJo software (TreeStar, Ashland, OR) was used to analyze flow cytometry data.

Antibodies	**Fluorophore**	**Suppliers**	**References**
CD117	BV785	Invitrogen	78-1171-82
Sca1	BV650	Invitrogen	64-5981-82
Lineage	AF700	Biolegend	799223
CD150	PeCy7	Biolegend	115914
CD48	PerCpCy5.5	Biolegend	103422

CD135	PeCy5	Biolegend	135312
CD34	AF647	BD biosciences	560230
IL-7 Ra	BV605	Biolegend	135041
Aqua Viability Dye	BV510	Invitrogen	L34957

Single-cell RNA sequencing

200,000 WBM cells from each mouse were pooled into groups and sequenced using the 10X Genomics Chromium Next GEM Single Cell 3' Kit v3.1 and Chip G kit and libraries were developed by the Stanford Functional Genomics Facility. Sequence alignment was performed using the mm10 (GSE63472) and 10X Genomics Cell Ranger V7 bioinformatics suite. Data were analyzed using R (version 4.3.0) and the Seurat package (version 2.3.1)[17]. For downstream analysis *FindVariableGenes* function was used to identify variable genes and *FindMarkersFunction* was used to identify differentially expressed genes. Moreover, pathway analysis was performed using *reactome* with *Griss J. ReactomeGSA* (https://github.com/reactome/ReactomeGSA (2019)) and gene set enrichment analysis was performed using *Enrichr* function[18].

Statistics

Statistical analyses were performed in R version 4.3.0 or Prism9 (GraphPad Software). Unpaired two-tailed t-test was used to define statistical significance (*P < 0.05, **P < 0.01, ***P < 0.001 and ****P < 0.0001).

Results

No short-term DNA damage post antagonistic anti-mCD117 mAb treatment was detected in wild-type or Fanconi Anemia mice.

To assess the short-term toxicity of antagonistic anti-mCD117 ACK2 mAb and investigate whether it can induce DNA damage, we conducted three different assays: colony formation counts (CFC), γH2AX analysis, and micronuclei assay.

Interestingly, at 7 days post- antagonistic anti-mCD117 mAb treatment in WT mice, we observed no significant differences in colony formation compared to the control groups (Figure 1A). However, we did observe an increase in the percentage of γH2AX-positive cells following antagonistic anti-mCD117 mAb treatment compared to the untreated and IgG-treated groups ($p<0.05$) (Figure 1B). To assess genome instability in mouse erythrocytes, we employed the micronuclei assay, which involves the identification of micronuclei (MN) in normochromatic erythrocytes (NCEs). These micronuclei are indicative of damage occurring more than 72 hours earlier and are identified by PI-positive and CD71-negative staining (supplementary Figure 1). Micronuclei assays are commonly used in toxicity studies to evaluate the potential carcinogenicity of substances and were used to assess potential risks associated with the antagonistic anti-mCD117 mAb[19]. Additionally, this assay allows us to determine the regenerative activity of the bone marrow during and after treatment. As previously reported, our results indicated that the percentage of reticulocytes (RETs) typically falls within the range of 1–3%. However, as expected, after 7 days, the reticulocyte count tended to increase following antagonistic anti-mCD117 mAb treatment, indicative of the bone marrow's ability to respond appropriately following disruption of its function. Moreover, no up-regulation of MN-NCE was detected following treatment. This reticulocyte response suggests that the bone marrow remains functional and possesses the necessary components to produce red blood cells after this BM insult (Figure 1C).

In contrast, in FANCD2$^{-/-}$ mice, we observed an upregulation in the number of colonies following the antagonistic anti-mCD117 mAb treatment compared to the control groups ($p<0.001$) (Figure 1D). This suggests that the antagonistic anti-mCD117 mAb may preferentially target HSCs with less self-renewal capability in this assay or alternatively that a progenitor response was elicited. Importantly, we did not detect any changes in γH2AX levels or the percentage of MN-NCEs, indicating that the antagonistic anti-mCD117 mAb does not induce DNA damage (Figure 1E, 1F).

To further explore the effects of the antagonistic anti-mCD117 mAb, we assessed changes in the number of long-term HSCs (LT-HSC: Lin- CD117+Sca1+CD150+CD48-), short-term HSCs (ST-HSC: Lin-CD117+Sca1+CD150-CD48-), and multipotent progenitors (MPP: Lin-

CD117+Sca1+CD150-CD48+) at the indicated time points post- antagonistic anti-mCD117 mAb or IgG mAb treatment compared to untreated groups using flow cytometry analysis (gating strategy; supplementary Figure 2). Surprisingly, we observed a decrease of the Lin-Sca1+Kit+ (LSK) population after both IgG and antagonistic anti-mCD117 mAb treatments in WT mice compared to the untreated group ($p<0.05$ and $p<0.01$, respectively) (Figure 2A). Additionally, within the LSK population, we detected an increase of ST-HSCs after IgG and antagonistic anti-mCD117 mAb treatments compared to the untreated group in WT mice, while no differences were detected in MPP and LT-HSC populations (Figure 2B, 2C, and 2D). This ST-HSC population up-regulation is indicative that the hematopoietic system is responding to overcome depletion once anti-mCD117 blockade is triggered. In contrast, focusing on FANCD2$^{-/-}$ mice, interestingly we observed no significant differences across the groups and subpopulations (Figure 2E, 2F, 2G, 2H). This observation indicates that one-time treatment of the anti-mCD117 mAb is not dramatically altering HSC or progenitor distribution in this setting.

No long-term DNA damage post antagonistic anti-mCD117 mAb treatment was detected in wild-type or Fanconi Anemia mice.

We additionally conducted an analysis at 24 weeks post-treatment aimed at uncovering potential long-term phenotypic and functional changes in residual/recovered hematopoietic stem and progenitor cells following antagonistic anti-mCD117 mAb treatment. Similar assays as those used at 1-week post-ACK2 mAb were employed. In both WT and FANCD2$^{-/-}$ mice, we did not identify differences between the groups at the 24-week time point (Figure 3).

Furthermore, the FACS analysis indicated a complete recovery in the percentage of LSK (Lin-Sca-1+c-Kit+) cells in WT mice after the antagonistic anti-mCD117 mAb treatment (Figure 4A). This finding supports the hypothesis that the antagonistic anti-mCD117 mAb does not have any adverse effects on the renewal capability of HSCs. Moreover, no significant differences were observed for other subpopulations following antagonistic anti-mCD117 mAb treatment (Figure 4B, 4C, and 4D). However, in the case of FANCD2$^{-/-}$ mice, we observed a slight increase of LSK and MPP following the antagonistic anti-mCD117 mAb treatment compared to the untreated group ($p<0.01$, $p<0.05$, Figure 4E, 4F), whereas ST-HSCs were decreased ($p<0.01$, Figure 4G). Interestingly, no significant differences were detected for the LT-HSCs subgroup (Figure 4H).

These findings indicate that the long-term effects of the antagonistic anti-mCD117 mAb treatment may lead to an increase in the number of LSK cells in the bone marrow of FANCD2$^{-/-}$ mice. This suggests that the antagonistic anti-mCD117 mAb may have eliminated the most dysregulated LSK cells, thereby allowing the other LSK pool with a higher renewal capability to compensate for this hematopoietic stress.

scRNA-seq analysis highlights the involvement of MAPK pathway with antagonistic anti-mCD117 mAb blockade.

To enhance our understanding of the antagonistic anti-mCD117 mAb effects and to ensure that it does not significantly alter long-term gene expression of the cells, we chose to perform scRNA-seq analysis on the WBM of untreated and ACK2-treated groups at 1-week and 24-weeks post-treatment in WT and FANCD2$^{-/-}$ mice. First, we determined the clustering of 14 cell subsets. We used an automated method using specific markers to identify each cluster[20]. This method allowed us to have the most probable subset for each of the clusters (supplementary figure 3). To probe deeper, we identified for each cluster the ten most expressed genes that allowed us to determine the cell identity according to the literature for each cluster[21]. For the myeloid component, we classified cells into monocytes (mainly expressing Ly6ca and Il1b), neutrophils (mainly expressing Mmp8, Mmp9, and Ly6g), macrophages (mainly expressing Csf1r and Klf4), and the myeloid progenitors into four subgroups using non-supervised clustering: Monocyte/Neutrophil progenitors and 1-3 myeloid progenitors (mainly expressing Cebpe, Elane, Mpo, and Csf1r), and dendritic cells (mainly expressing Siglech and Irf8). In the lymphoid component, focusing on B cells, we identified four different subsets: B-cell progenitors, immature B cells, B cells and plasma cells (mainly expressing Pax5, Ebf1, and Iglc1). We also identified common lymphoid progenitors (CLP, mainly expressing Lck, Tox, and Prkch). The last cluster was related to erythroblasts (Hbb-bs, Hba-a1, and Hba-a2) (supplementary figure 4A, 4B, and 4C). We subdivided the data by condition to determine the distribution of each cluster (supplementary figure 4D).

To delve further, we first conducted an analysis of the 100 pathways with the maximum difference in expression across samples using *ReactomeGSA* package. No drastic changes or pathway activations were found between all samples (supplementary figure 5). We conducted a second non-supervised analysis using *WikiPathways_2019_Mouse data base* to identify which

pathways were most upregulated and downregulated after the antagonistic anti-mCD117 mAb treatment compared to the control for each group. Using this assessment, several pathways were found to be affected. Notably, we found that the MAPK signaling pathway ranked as the second and third most downregulated pathway 1 week after the antagonistic anti-mCD117 mAb treatment for WT mice and FANCD2-/- mice, respectively (supplementary figure 6A, 6B). To assess if this downregulation was reversible, we conducted the same analysis at 24 weeks post-antagonistic anti-mCD117 mAb treatment. Surprisingly, we found that the MAPK pathway was upregulated in WT mice, supporting the hypothesis that the antagonistic anti-mCD117 mAb treatment is not permanently impacting this pathway in the hematopoietic cells (supplementary figure 6C, 6D).

To probe further, we decided to explore and conduct an analysis of differential gene expression between untreated and treated groups, considering different time points and mouse strains for each cluster. From this analysis, we selected all genes that were upregulated or downregulated with a *p-value* < 0.05 and an average log2 fold change (avg_log2FC) < ±0.5 for each cluster (supplementary table 1). Subsequently, we created Venn diagrams for each cluster to investigate if genes were commonly upregulated or downregulated following antagonistic anti-mCD117 mAb treatment (supplementary figures 7-20). Interestingly, we observed across clusters that Fos was significantly downregulated 1-week after treatment in both WT and FANCD2$^{-/-}$ mice whereas at 24-weeks post-treatment in WT mice Fos was upregulated (supplementary figures 7-20).

Considering that CD117 (c-Kit) is known to be involved in the activation of various signaling pathways, such as the MAPK pathway, and that Fos is associated with MAPK activation as a transcription factor, we decided to examine the activation of the genes associated to this pathway. We found that accordingly with our previous results that Fos and Jun are downregulated post antagonistic anti-mCD117 at 1 week for both mice models. Moreover, we assessed other genes associated to PI3K/AKT, JAK2/STAT5, Src or PKC pathways and only Pi3k has differential expression between group. More precisely, it is upregulated post antagonistic anti-mCD117 mAb at 1 week in both mice models (supplementary figure 6E).

This data provides evidence that antagonistic anti-mCD117 ACK2 mAb, by blocking c-Kit, disrupts the MAPK pathway and downregulates the expression of the Fos/Jun transcription factors, overcome by the activation of PI3K/AKT pathway (supplementary figure 6F).

Discussion

The use of a targeted antibody to deplete host HSCs before transplantation in patients with hematopoietic diseases such as FA is one of the first promising alternative treatments to chemotherapy or radiotherapy[10]. We elucidated the safety of antagonistic anti-CD117 mAb-mediated BMT/HSCT in both WT and FA mice with the specific goal to generate biological insights clarifying the vulnerability of HSCs to antagonistic anti-mCD117 ACK2-mediated Stem Cell Factor (SCF)-CD117 proliferative signaling blockade and additionally to provide pre-clinical toxicity analysis of antagonistic anti-CD117 mAbs to assess safety and aid in clinical development. Given the increased sensitivity of FA patients to genotoxic and proliferative stressors and potential for resulting mixed chimerism with this approach, these experiments are of paramount importance to inform potential future clinical studies for this patient group. The effects of antagonistic anti-mouse CD117 mAb-ACK2 treatment were compared to untreated and IgG mAb mock-treated WT or FANCD2$^{-/-}$ mutant mice 1-week and 24-weeks post mAb treatment. We elucidated the short- and long-term safety of the antagonistic anti-mCD117 ACK2 mAb and showed that no drastic cellular stress or DNA damage where generated which could lead to MDS induction in long-term. This result indicated that the antagonistic anti-mCD117 ACK2 mAb is not producing a selective pressure of clonal proliferation cells which could predispose to MDS.

Our research, along with the work of our colleagues, has demonstrated that a single treatment with the antagonistic anti-mCD117 mAb ACK2 can selectively deplete host HSCs *in vivo*, thereby facilitating effective engraftment of donor hematopoietic cells in syngeneic immunodeficient murine models. However, it is important to note that ACK2 mAb alone does not enhance donor engraftment in WT hosts and currently has limited conditioning efficacy in this setting, making it primarily applicable to specific genetic disease contexts currently. Notably, recent reports have highlighted the effectiveness of antagonistic anti-mCD117 ACK2 mAb as a pre-transplant conditioning agent in FA mouse models in combination with immunosuppression. Specifically, when ACK2 mAb treatment is combined with anti-CD4 mAb (GK1.5), it has enabled remarkable long-term, multi-lineage donor engraftment, reaching up to 63% and 93% in homozygous mutant FANCA$^{-/-}$ and FANCD2$^{-/-}$ recipients post- BMT respectively[13].

Recently our laboratory conducted similar experiments to assess the conditioning capacity of antagonistic anti-mCD117 ACK2 mAb in combination with GK1.5 in FANCD2$^{-/-}$ animals[14]. We chose the FANCD2$^{-/-}$ model for these studies due to its well-established severe hematopoietic phenotype, which aligns with prior investigations. Our preliminary results, we also observed that pre-treatment with ACK2 and anti-mCD4 GK1.5 mAb enabled engraftment of WT donor HSCs in FANCD2$^{-/-}$ animals. This finding supports the hypothesis that ACK2 mAb may facilitate the depletion of host FANCD2$^{-/-}$ HSCs, thereby promoting successful donor HSCT. Furthermore, our detailed analysis of these studies suggests that the proliferative and hematopoietic reconstitution capacity of WT donor HSCs and HSPCs can outcompete FANCD2$^{-/-}$ host HSPCs over time which was also accomplished with anti-mCD4 GK1.5 mAb alone. This competition leads to high levels of donor hematopoietic chimerism in both the BM and peripheral blood. In line with successful donor hematopoietic engraftment in this experiment, we observed an increase in progenitor cells with functional ICL repair activity post-conditioned transplantation, as demonstrated by *in vitro* CFC assays in the presence of Mitomycin C.

However, our results also indicate that a significant population of FANCD2$^{-/-}$ HSCs remain in the host long term, resulting in a state of mixed hematopoietic chimerism. This mixed chimerism raises potential concerns in the context of FA, as residual host HSCs, subjected to additional hematopoietic stress through antibody based HSCT, might be predisposed to malignant transformation. While our studies did not report any evidence of MDS or leukemia development in the antagonistic anti-mCD117 mAb ACK2-conditioned FA animals that underwent BMT understanding the extent of antagonistic anti-mCD117 mAb ACK2-induced hematopoietic stress and DNA damage remains of critical importance. Importantly, prior reports indicate epithelial tumor development in FANCD2-/- model between 14 - 19 months of age, but hematologic malignancies have not been observed in this model[22].

Furthermore, our scRNA-seq data analysis has revealed the inhibition of the MAPK pathway and the downregulation of the transcription factor Fos as a consequence of antagonistic anti-mCD117 ACK2 mAb blocking the c-Kit/SCF axis. These findings are the first to shed light on the potential action of antagonistic anti-mCD117 ACK2 mAb. Previous studies have underscored the pivotal role of the MAPK pathway in regulating HSC quiescence[23–25]. Indeed, the MAPK signaling pathway is instrumental in promoting cell proliferation by activating cyclin-CDK complexes, thereby facilitating cell cycle progression and gene transcription. Additionally, this

pathway exerts its influence on various transcriptional regulators, further bolstering its involvement in the regulation of cellular proliferation. It is worth noting that several tyrosine kinase inhibitors known for their ability to target c-Kit -- such as Imatinib, Sunitinib, or Dasatinib -- have been extensively characterized and used in the context of cancer therapy, primarily for their anti-proliferative effects. Our results suggest that the antagonistic anti-mCD117 ACK2 mAb may induce a similar effect by specifically targeting c-Kit on cells that overexpress it. This highlights the potential therapeutic implications of antagonistic anti-CD117 mAbs in modulating c-Kit-mediated signaling pathways and cellular proliferation.

Our research signifies a significant advance in the understanding of the safety and efficacy of HSC-targeted antibody-based therapies with a focus on bone marrow failure conditions, offering hope for improved treatments in the future for these patients. The potential benefits and insights gained from this study underscore the importance of continued investigation into the clinical utility of antagonistic anti-CD117 mAbs for FA and related disorders. This discovery has prompted efforts to translate these findings into clinical applications to evaluate the potential adoption of this conditioning approach for FA patients. Based upon these reassuring results, we have recently opened a clinical trial to test the use of antagonistic anti-CD117 mAb conditioning in FA patients in combination with transient immunosuppression and TCRαβ+ T-Cell/CD19+ B-Cell depleted grafts thereby eliminating the use of total body irradiation or busulfan from the conditioning regimen of these high-risk patients (NCT04784052). Further, antagonistic anti-CD117 mAb treatment is being utilized in a number of other conditions and insights into its effects on hematopoiesis may be pertinent to other settings as well.

References

1. Khan NE, Rosenberg PS, Alter BP. Preemptive Bone Marrow Transplantation and Event-Free Survival in Fanconi Anemia. Biol Blood Marrow Transplant. 2016;22(10):1888-1892.

2. Nebert DW, Dong H, Bruford EA, Thompson DC, Joenje H, Vasiliou V. Letter to the editor for "Update of the human and mouse Fanconi anemia genes". Hum Genomics. 2016;10(1):25.

3. Dufour C, Pierri F. Modern management of Fanconi anemia. Hematology Am Soc Hematol Educ Program. 2022;2022(1):649-657.

4. Ebens CL, MacMillan ML, Wagner JE. Hematopoietic cell transplantation in Fanconi anemia: current evidence, challenges and recommendations. Expert Rev Hematol. 2017;10(1):81-97.

5. Fink O, Even-Or E, Avni B, et al. Two decades of stem cell transplantation in patients with Fanconi anemia: Analysis of factors affecting transplant outcomes. Clin Transplant. 2023;37(1):e14835.

6. MacMillan ML, DeFor TE, Young J-AH, et al. Alternative donor hematopoietic cell transplantation for Fanconi anemia. Blood. 2015;125(24):3798-3804.

7. Rosenberg PS, Socié G, Alter BP, Gluckman E. Risk of head and neck squamous cell cancer and death in patients with Fanconi anemia who did and did not receive transplants. Blood. 2005;105(1):67-73.

8. Peffault de Latour R, Porcher R, Dalle J-H, et al. Allogeneic hematopoietic stem cell transplantation in Fanconi anemia: the European Group for Blood and Marrow Transplantation experience. Blood. 2013;122(26):4279-4286.

9. Bhattacharya D, Czechowicz A, Ooi AGL, Rossi DJ, Bryder D, Weissman IL. Niche recycling through division-independent egress of hematopoietic stem cells. J Exp Med. 2009;206(12):2837-2850.

10. Czechowicz A, Kraft D, Weissman IL, Bhattacharya D. Efficient transplantation via antibody-based clearance of hematopoietic stem cell niches. Science. 2007;318(5854):1296-1299.

11. Logan AC, Czechowicz A, Kelley BV, et al. Anti-CD117 (c-Kit) Monoclonal Antibodies Deplete Human Hematopoietic Stem Cells and Facilitate Their Replacement in Humanized NOD/SCID/IL2Rγ−/− Mice: A Non-Toxic Conditioning Regimen for Allotransplantation. Blood. 2012;120(21):4099.

12. Czechowicz A, Bhardwaj R, Pang W, Park CY, Weissman IL. Targeted Clearance of Human Hematopoietic Stem Cell Niches Via Inhibition of SCF Signaling Using Monoclonal Antibody SR-1. Biol Blood Marrow Transplant. 2011;17(2):S187-S188.

13. Chandrakasan S, Jayavaradhan R, Ernst J, et al. KIT blockade is sufficient for donor hematopoietic stem cell engraftment in Fanconi anemia mice. Blood. 2017;129(8):1048-1052.

14. Chan YY, Ho PY, Swartzrock L, et al. Non-genotoxic Restoration of the Hematolymphoid System in Fanconi Anemia. Transplant Cell Ther. 2023;29(3):164.e1-164.e9.

15. Houghtaling S, Timmers C, Noll M, et al. Epithelial cancer in Fanconi anemia complementation group D2 (Fancd2) knockout mice. Genes Dev. 2003;17(16):2021-2035.

16. Balmus G, Karp NA, Ng BL, Jackson SP, Adams DJ, McIntyre RE. A high-throughput in vivo micronucleus assay for genome instability screening in mice. Nat Protoc. 2015;10(1):205-215.

17. Butler A, Hoffman P, Smibert P, Papalexi E, Satija R. Integrating single-cell transcriptomic data across different conditions, technologies, and species. Nat Biotechnol. 2018;36(5):411-420.

18. Kuleshov MV, Jones MR, Rouillard AD, et al. Enrichr: a comprehensive gene set enrichment analysis web server 2016 update. Nucleic Acids Res. 2016;44(W1):W90-97.

19. Hayashi M. The micronucleus test-most widely used in vivo genotoxicity test. Genes Environ. 2016;38:18.

20. Ianevski A, Giri AK, Aittokallio T. Fully-automated and ultra-fast cell-type identification using specific marker combinations from single-cell transcriptomic data. Nat Commun. 2022;13(1):1246.

21. Baccin C, Al-Sabah J, Velten L, et al. Combined single-cell and spatial transcriptomics reveal the molecular, cellular and spatial bone marrow niche organization. Nat Cell Biol. 2020;22(1):38-48.

22. Parmar K, D'Andrea A, Niedernhofer LJ. Mouse models of Fanconi anemia. Mutat Res. 2009;668(1-2):133-140.

23. Ito K, Hirao A, Arai F, et al. Reactive oxygen species act through p38 MAPK to limit the lifespan of hematopoietic stem cells. Nat Med. 2006;12(4):446-451.

24. Jang Y-Y, Sharkis SJ. A low level of reactive oxygen species selects for primitive hematopoietic stem cells that may reside in the low-oxygenic niche. Blood. 2007;110(8):3056-3063.

25. Geest CR, Coffer PJ. MAPK signaling pathways in the regulation of hematopoiesis. J Leukoc Biol. 2009;86(2):237-250.

26. Pico AR, Kelder T, Iersel MP van, Hanspers K, Conklin BR, Evelo C. WikiPathways: Pathway Editing for the People. PLoS Biol. 2008;6(7):e184.

Figure 1: No acute DNA damage was detected after antagonistic anti-CD117 mAb treatment in FANCD2-/- mice. A-C: WT mice, (A) Functional assessment by in vitro colony forming capacity. (B) yH2AX detection percentage by immunofluorescence. (C) Micronuclei assay analysis representing percentage of reticulocytes (RET) and micronuclei (MN)-RET. D-F: FANCD2-/- mice (D) Functional assessment by in vitro colony forming capacity. (E) yH2AX detection percentage by immunofluorescence. (F) Micronuclei assay analysis representing percentage of RET and MN-RET. Data shown are mean values and error bars are ± SEM. n= 3 to 5 mice per group: *, P<0.05; ****, P < 0.0001, using Mann–Whitney t-test.

Figure 2: Impact on hematopoietic stem and progenitor cells assessed by flow cytometry at 1 week post administration of IgG and antagonistic anti-CD117 mAb. A-D: WT mice, E-H: FANCD2-/- mice. (A/E) Histograms represent the percentage of LSK cells in the lin- fraction, (B/F) Histograms represent the percentage of MPP cells in the LSK cell fraction, (C/G) Histograms represent the percentage of ST-HSC cells in the LSK cell fraction, (D/H) Histograms represent the percentage of LT-HSC cells in the LSK cell fraction. Data shown are mean values and error bars are ± SEM. n=5 mice per group: *, P < 0.05; **, P < 0.01, using Mann–Whitney t-test.

Figure 3: No long-term DNA damage was detected after antagonistic anti-CD117 mAb treatment in FANCD2-/- mice. A-C: WT mice, (A) Functional assessment by in vitro colony forming capacity. (B) yH2AX detection percentage by immunofluorescence. (C) Micronuclei assay analysis representing percentage of RET and MN-RET. D-F: FANCD2-/- mice (D) Functional assessment by in vitro colony forming capacity. (E) yH2AX detection percentage by immunofluorescence. (F) Micronuclei assay analysis representing percentage of RET and MN-RET. Data shown are mean values and error bars are ± SEM. n=2 to 5 mice per group: no significant difference was detected using Mann–Whitney t-test.

Figure 4: Impact on hematopoietic stem and progenitor cells assessed by flow cytometry at 24 weeks post administration of IgG and antagonistic anti-CD117 mAb. A-D: WT mice, E-H: FANCD2-/- mice. (A/E) Histograms represent the percentage of LSK cells in the lin- fraction, (B/F) Histograms represent the percentage of MPP cells in the LSK cell fraction, (C/G) Histograms represent the percentage of ST-HSC cells in the LSK cell fraction, (D/H) Histograms represent the percentage of LT-HSC cells in the LSK cell fraction. Data shown are mean values and error bars are ± SEM. n=2 to 5 mice per group: *, P < 0.05; **, P < 0.01, using Mann–Whitney t-test.

Figure 1

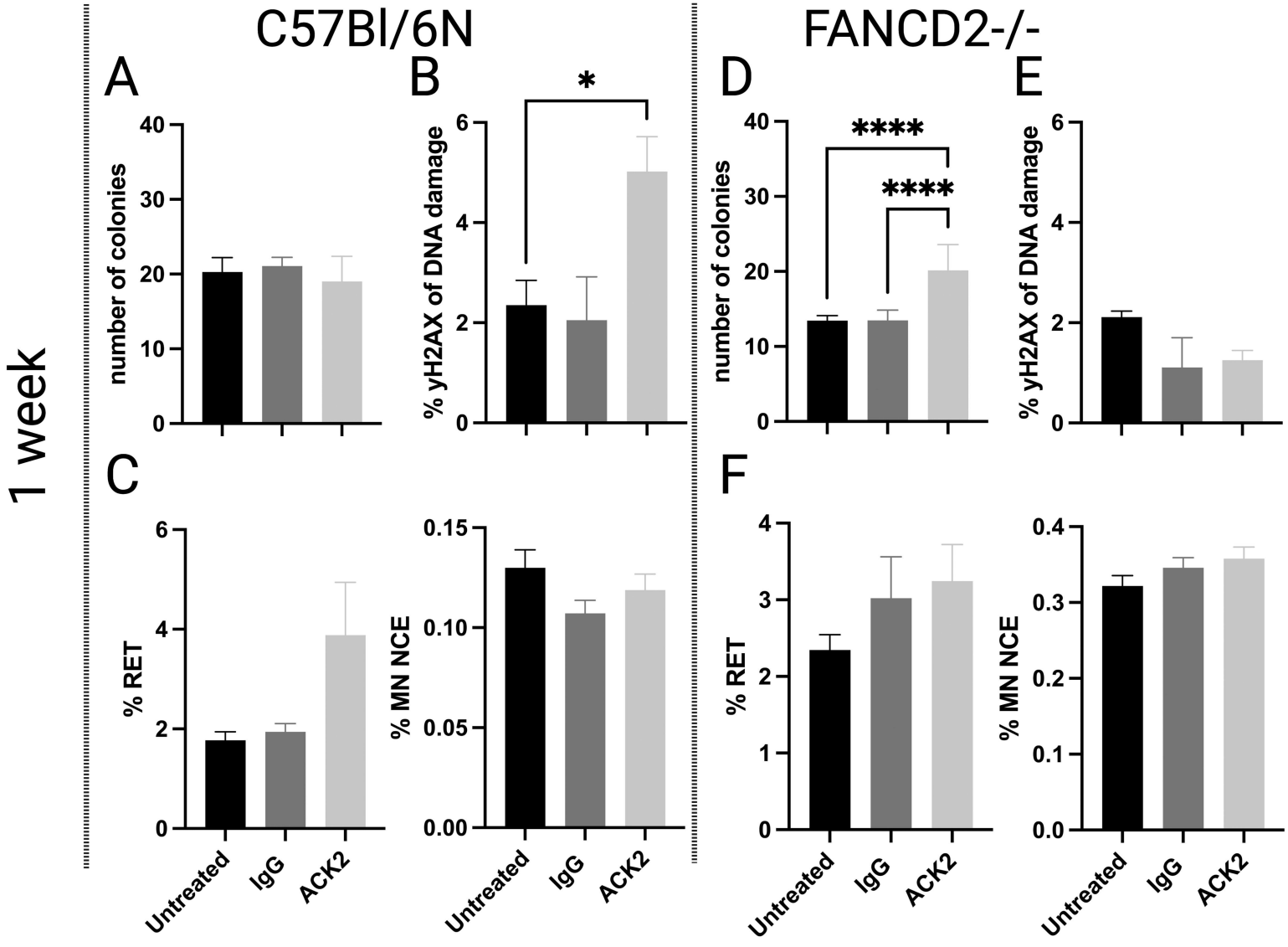
1 week
C57Bl/6N
FANCD2-/-
A
B
C
D
E
F
number of colonies
% yH2AX of DNA damage
% RET
% MN NCE
*
****
****
Untreated
IgG
ACK2

Figure 2

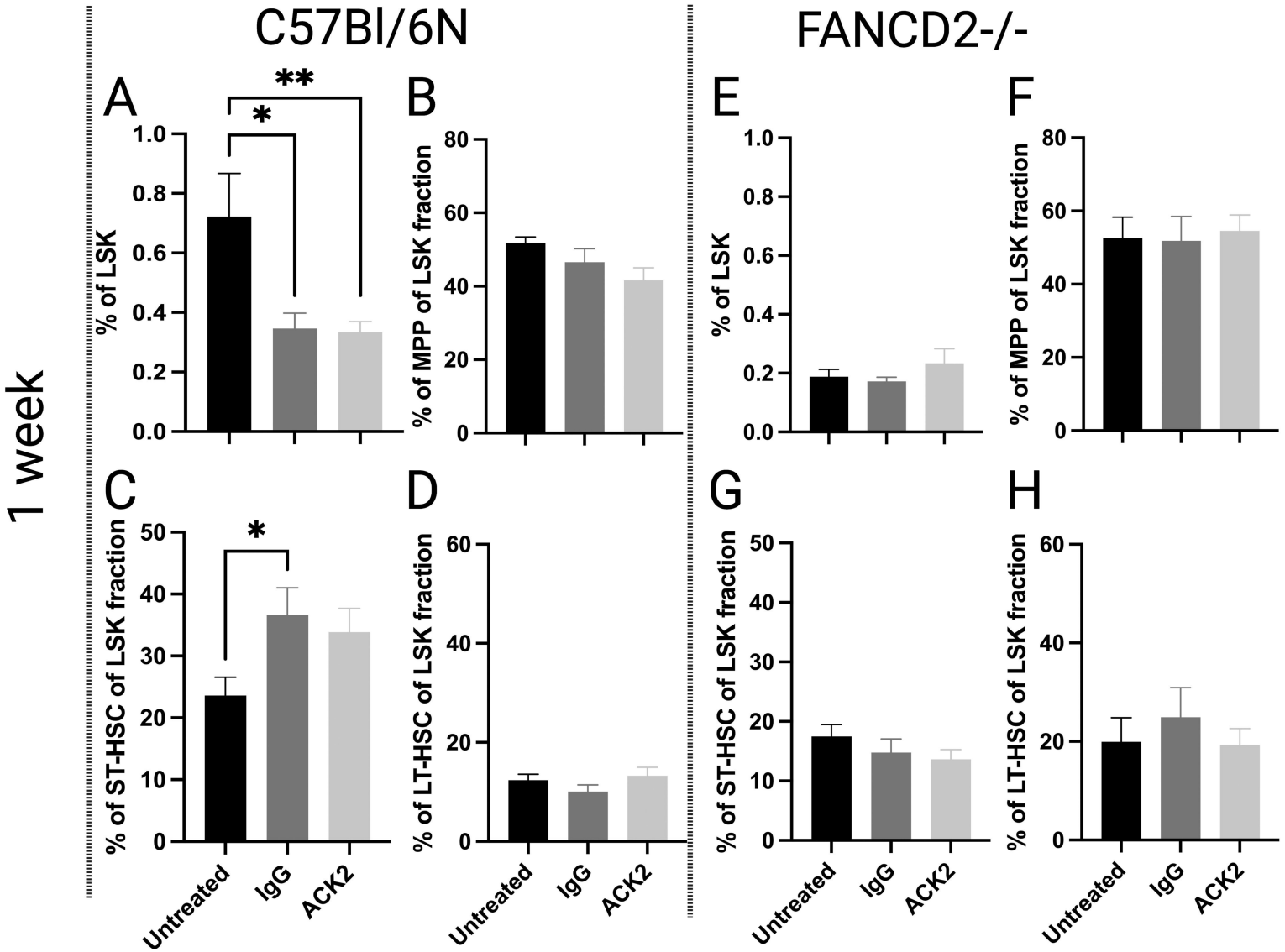
C57Bl/6N
FANCD2-/-
1 week
A
B
C
D
E
F
G
H
% of LSK
% of MPP of LSK fraction
% of ST-HSC of LSK fraction
% of LT-HSC of LSK fraction
*
**
Untreated
IgG
ACK2

Figure 3

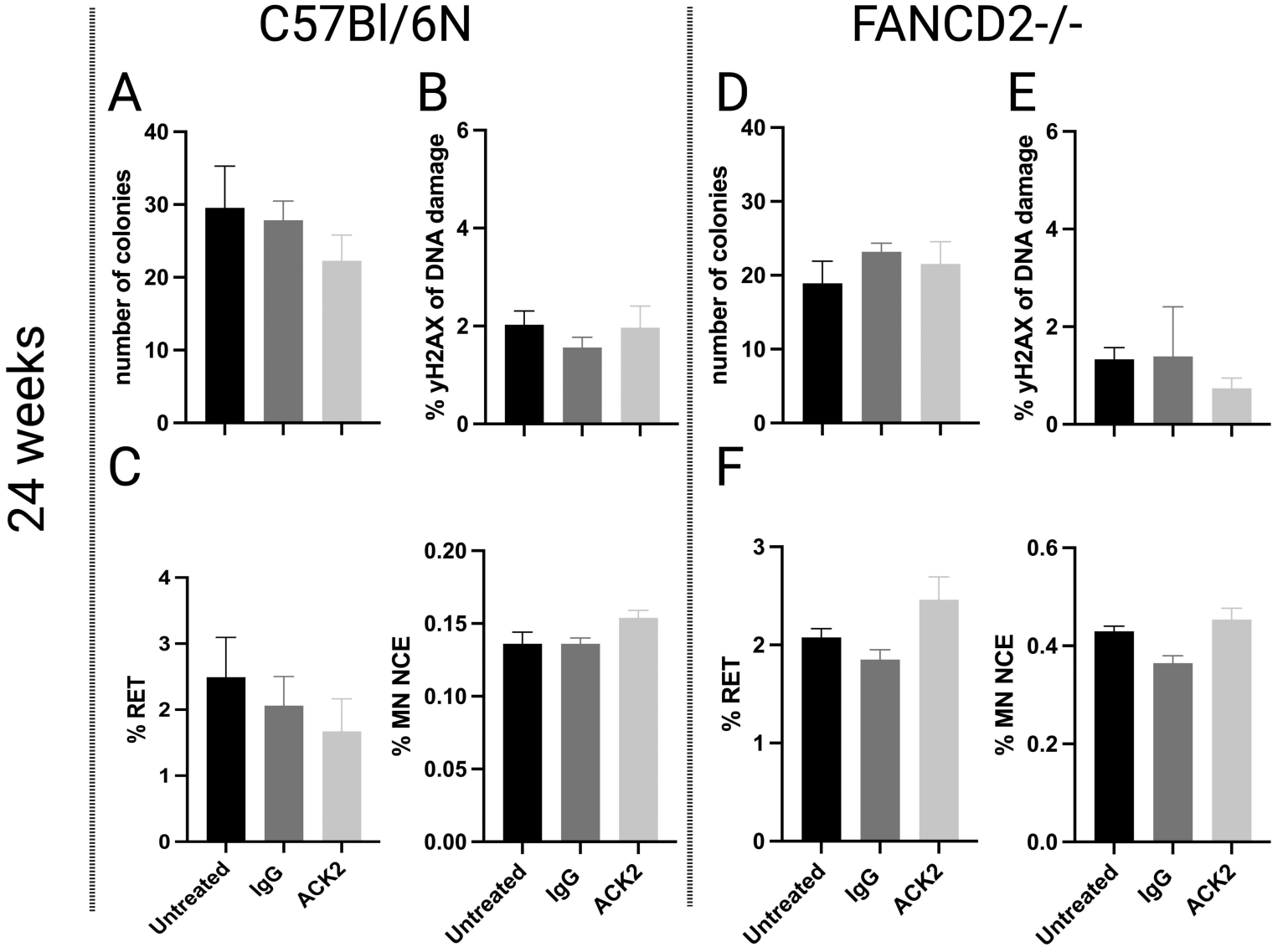
C57Bl/6N
FANCD2-/-
24 weeks
A
B
C
D
E
F
number of colonies
% yH2AX of DNA damage
% RET
% MN NCE
Untreated
IgG
ACK2

Figure 4

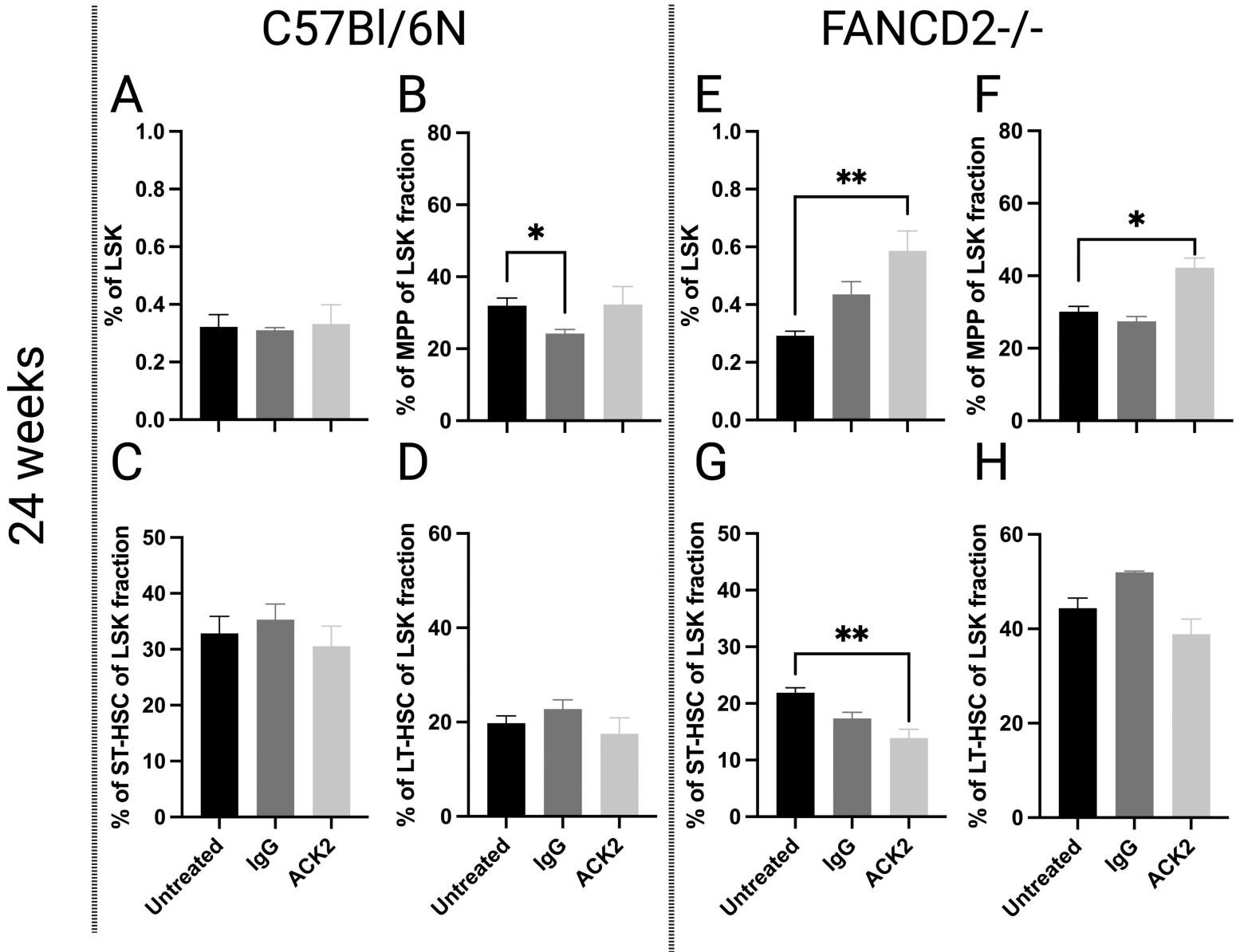
24 weeks
C57Bl/6N
FANCD2-/-
A
B
E
F
C
D
G
H
% of LSK
% of MPP of LSK fraction
% of ST-HSC of LSK fraction
% of LT-HSC of LSK fraction
*
**
Untreated
IgG
ACK2

Supplementary Table 1: Untreated group compared with treated group genes upregulated or downregulated for each cluster. (See Excel file)

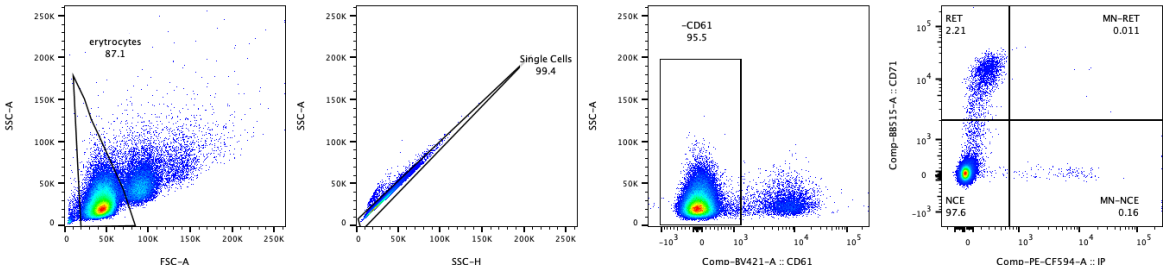

Supplementary Figure 1: FACS plot representative of the gating strategy used following micronuclei assay staining.

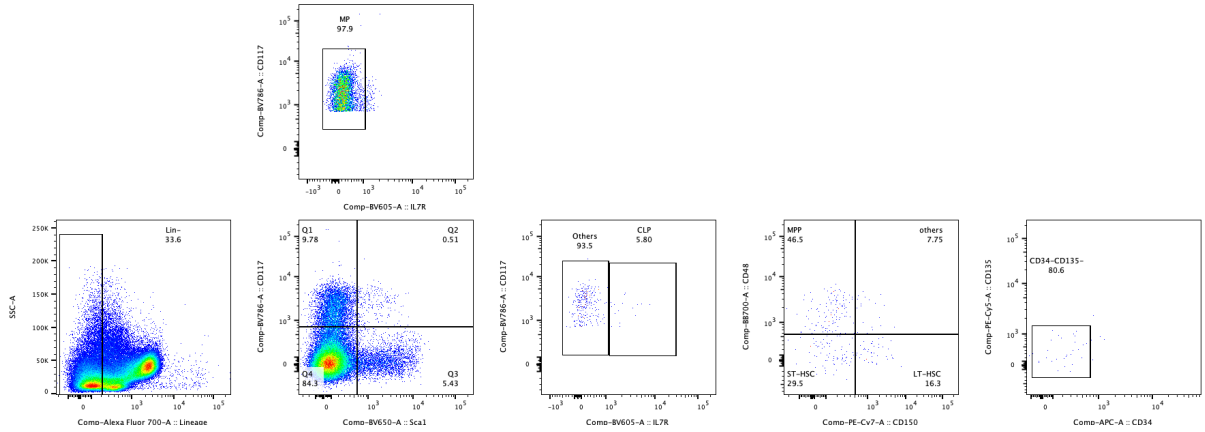

Supplementary Figure 2: FACS plot representative of the gating strategy following staining.

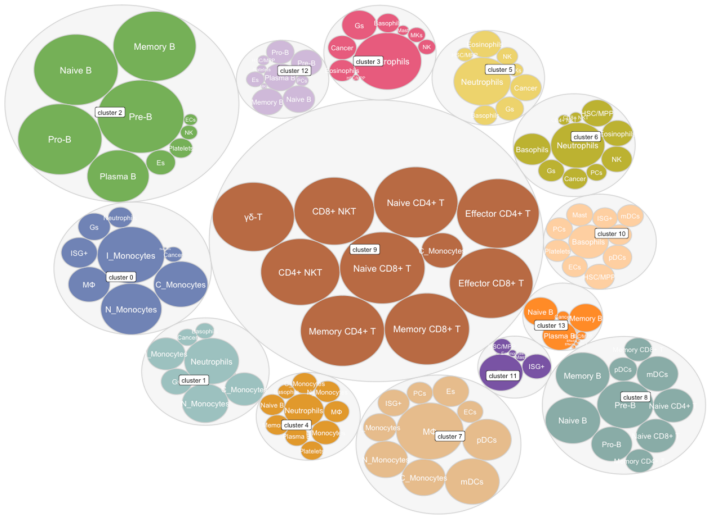

Supplementary Figure 3: Bubble plot showing all the cell types that were considered as the most probable by ScType for cluster annotation.

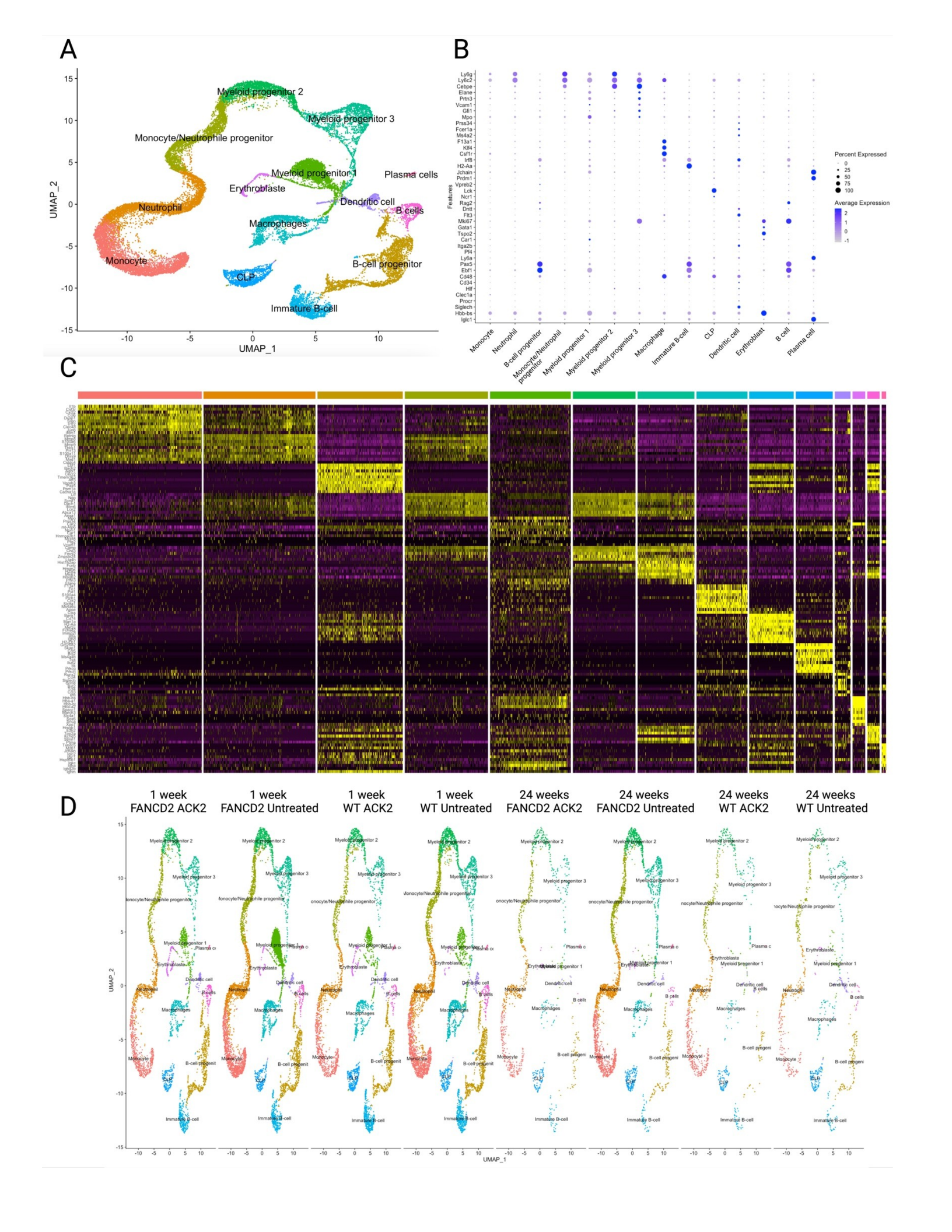
A
Myeloid progenitor 2
Myeloid progenitor 3
Monocyte/Neutrophile progenitor
Myeloid progenitor 1
Plasma cells
Erythroblaste
Dendritic cell
Neutrophil
B cells
Macrophages
Monocyte
B-cell progenitor
CLP
Immature B-cell
UMAP_1
UMAP_2
B
Percent Expressed
Average Expression
Features
Monocyte
Neutrophil
B-cell progenitor
Monocyte/Neutrophil progenitor
Myeloid progenitor 1
Myeloid progenitor 2
Myeloid progenitor 3
Macrophage
Immature B-cell
CLP
Dendritic cell
Erythroblast
B cell
Plasma cell
C
D
1 week FANCD2 ACK2
1 week FANCD2 Untreated
1 week WT ACK2
1 week WT Untreated
24 weeks FANCD2 ACK2
24 weeks FANCD2 Untreated
24 weeks WT ACK2
24 weeks WT Untreated
UMAP_1
UMAP_2

Supplementary Figure 4: Integrated analysis for each group and identification of sub-clusters of distinct cell types. (A) UMAP of concatenate sample. The UMAP embedding and Leiden clustering were performed on the integrated gene expression, Cells are labeled based on their cluster identity. (B) Dot plot showing the average expression of selected marker genes for each cluster. The size of dots represents the fraction of cells expressing a given gene (>0 expression value) and the color intensity reflects the average expression level within each cluster. (C) Heatmap of cluster signature genes highlighted on left. Expression of the 10 top differentially expressed genes across the cells. (D) UMAP split by samples representing the distribution of cells by cluster.

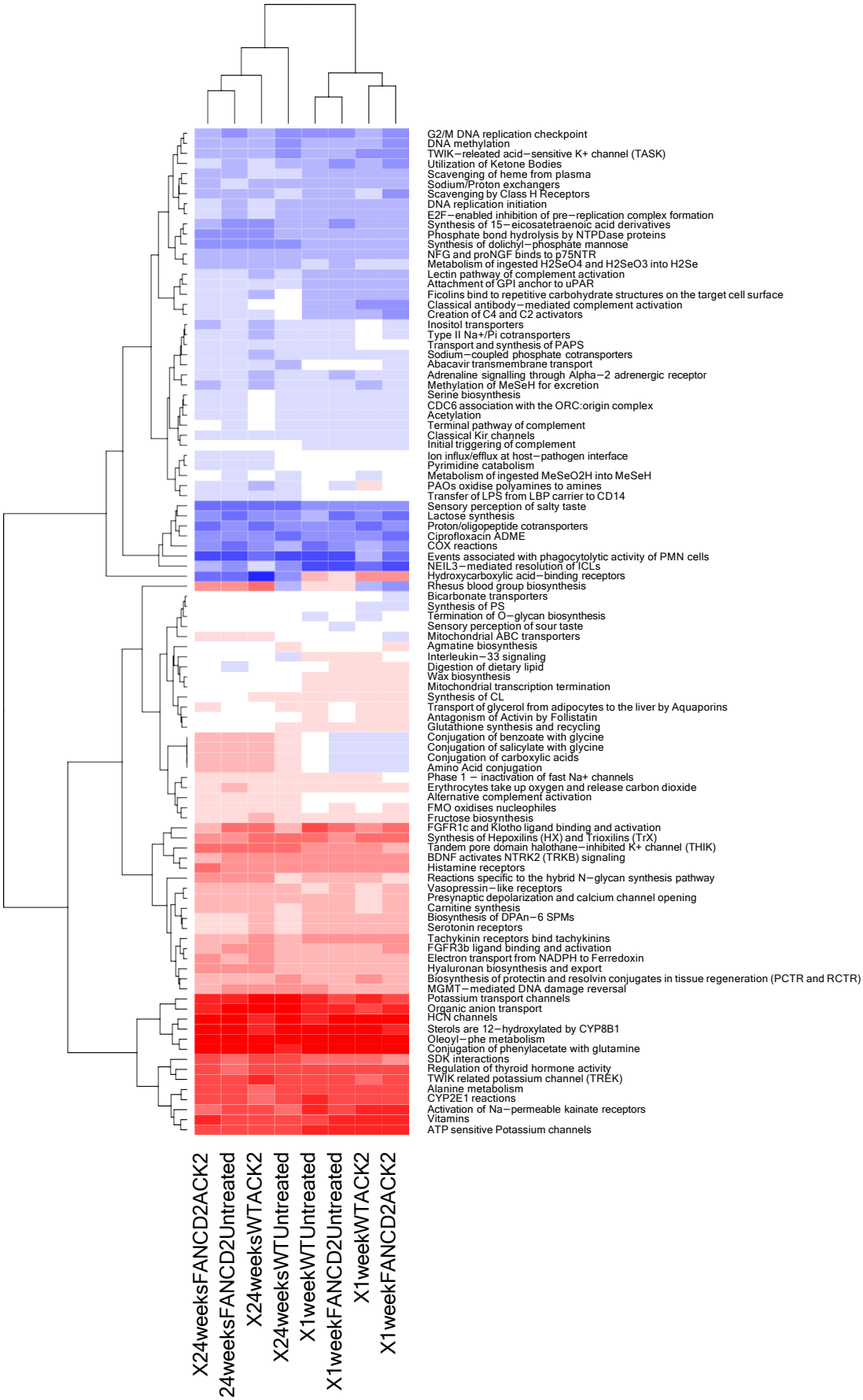

Supplementary Figure 5: Heatmap of the top 100 differential pathways by Reactome gene set analysis.

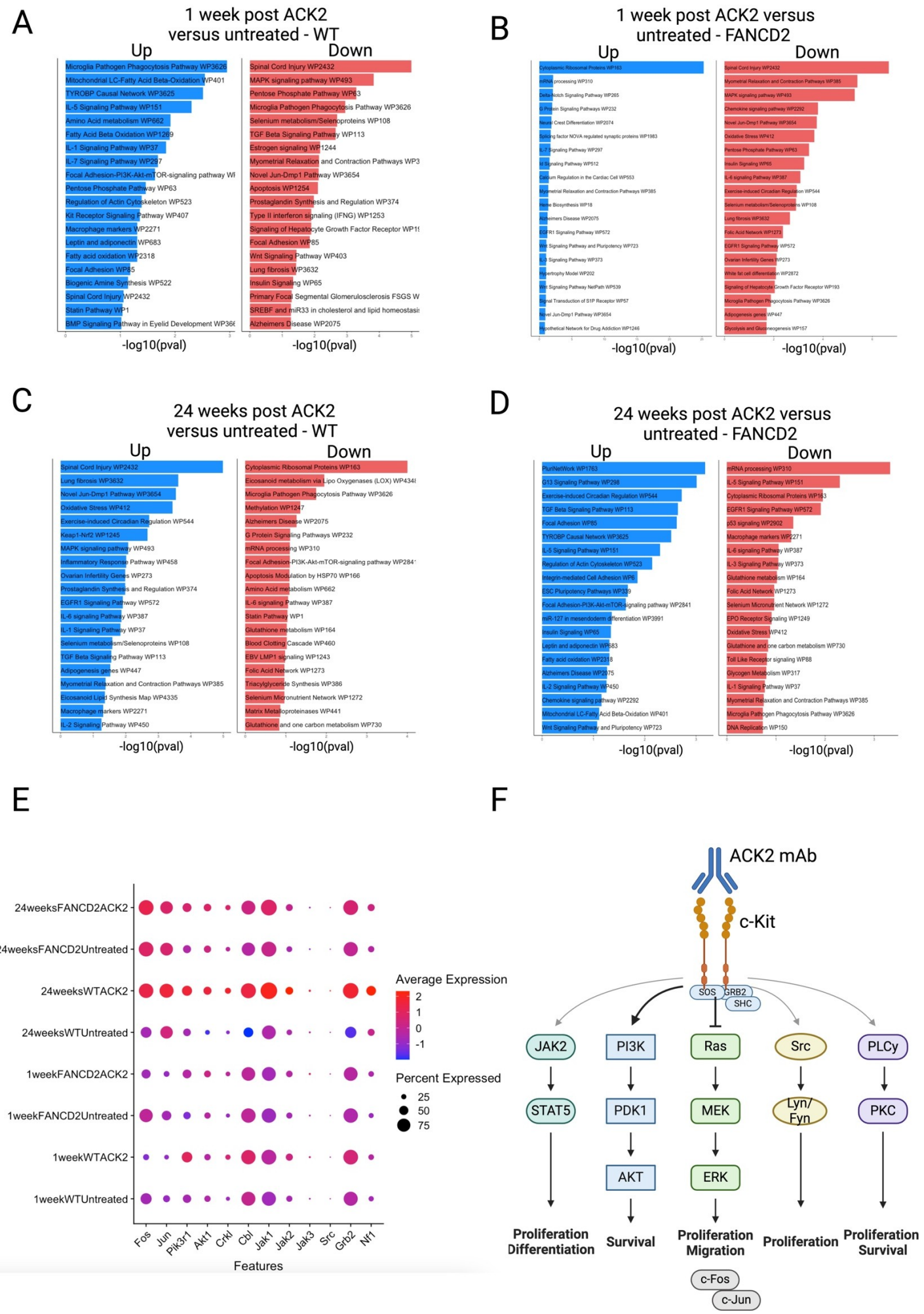
A
1 week post ACK2 versus untreated - WT
Up
Down
Microglia Pathogen Phagocytosis Pathway WP3626
Mitochondrial LC-Fatty Acid Beta-Oxidation WP401
TYROBP Causal Network WP3625
IL-5 Signaling Pathway WP151
Amino Acid metabolism WP662
Fatty Acid Beta Oxidation WP1269
IL-1 Signaling Pathway WP37
IL-7 Signaling Pathway WP297
Focal Adhesion-PI3K-Akt-mTOR-signaling pathway WI
Pentose Phosphate Pathway WP63
Regulation of Actin Cytoskeleton WP523
Kit Receptor Signaling Pathway WP407
Macrophage markers WP2271
Leptin and adiponectin WP683
Fatty acid oxidation WP2318
Focal Adhesion WP85
Biogenic Amine Synthesis WP522
Spinal Cord Injury WP2432
Statin Pathway WP1
BMP Signaling Pathway in Eyelid Development WP36
Spinal Cord Injury WP2432
MAPK signaling pathway WP493
Pentose Phosphate Pathway WP63
Microglia Pathogen Phagocytosis Pathway WP3626
Selenium metabolism/Selenoproteins WP108
TGF Beta Signaling Pathway WP113
Estrogen signaling WP1244
Myometrial Relaxation and Contraction Pathways WP3
Novel Jun-Dmp1 Pathway WP3654
Apoptosis WP1254
Prostaglandin Synthesis and Regulation WP374
Type II interferon signaling (IFNG) WP1253
Signaling of Hepatocyte Growth Factor Receptor WP1
Focal Adhesion WP85
Wnt Signaling Pathway WP403
Lung fibrosis WP3632
Insulin Signaling WP65
Primary Focal Segmental Glomerulosclerosis FSGS W
SREBF and miR33 in cholesterol and lipid homeostasis
Alzheimers Disease WP2075
-log10(pval)
-log10(pval)
B
1 week post ACK2 versus untreated - FANCD2
Up
Down
Cytoplasmic Ribosomal Proteins WP163
mRNA processing WP310
Delta-Notch Signaling Pathway WP265
G Protein Signaling Pathways WP232
Neural Crest Differentiation WP2074
Splicing factor NOVA regulated synaptic proteins WP1983
IL-7 Signaling Pathway WP297
Id Signaling Pathway WP512
Calcium Regulation in the Cardiac Cell WP553
Myometrial Relaxation and Contraction Pathways WP385
Heme Biosynthesis WP18
Alzheimers Disease WP2075
EGFR1 Signaling Pathway WP572
Wnt Signaling Pathway and Pluripotency WP723
IL-3 Signaling Pathway WP373
Hypertrophy Model WP202
Wnt Signaling Pathway NetPath WP539
Signal Transduction of S1P Receptor WP57
Novel Jun-Dmp1 Pathway WP3654
Hypothetical Network for Drug Addiction WP1246
Spinal Cord Injury WP2432
Myometrial Relaxation and Contraction Pathways WP385
MAPK signaling pathway WP493
Chemokine signaling pathway WP2292
Novel Jun-Dmp1 Pathway WP3654
Oxidative Stress WP412
Pentose Phosphate Pathway WP63
Insulin Signaling WP65
IL-6 signaling Pathway WP387
Exercise-induced Circadian Regulation WP544
Selenium metabolism/Selenoproteins WP108
Lung fibrosis WP3632
Folic Acid Network WP1273
EGFR1 Signaling Pathway WP572
Ovarian Infertility Genes WP273
White fat cell differentiation WP2872
Signaling of Hepatocyte Growth Factor Receptor WP193
Microglia Pathogen Phagocytosis Pathway WP3626
Adipogenesis genes WP447
Glycolysis and Gluconeogenesis WP157
-log10(pval)
-log10(pval)
C
24 weeks post ACK2 versus untreated - WT
Up
Down
Spinal Cord Injury WP2432
Lung fibrosis WP3632
Novel Jun-Dmp1 Pathway WP3654
Oxidative Stress WP412
Exercise-induced Circadian Regulation WP544
Keap1-Nrf2 WP1245
MAPK signaling pathway WP493
Inflammatory Response Pathway WP458
Ovarian Infertility Genes WP273
Prostaglandin Synthesis and Regulation WP374
EGFR1 Signaling Pathway WP572
IL-6 signaling Pathway WP387
IL-1 Signaling Pathway WP37
Selenium metabolism/Selenoproteins WP108
TGF Beta Signaling Pathway WP113
Adipogenesis genes WP447
Myometrial Relaxation and Contraction Pathways WP385
Eicosanoid Lipid Synthesis Map WP4335
Macrophage markers WP2271
IL-2 Signaling Pathway WP450
Cytoplasmic Ribosomal Proteins WP163
Eicosanoid metabolism via Lipo Oxygenases (LOX) WP434
Microglia Pathogen Phagocytosis Pathway WP3626
Methylation WP1247
Alzheimers Disease WP2075
G Protein Signaling Pathways WP232
mRNA processing WP310
Focal Adhesion-PI3K-Akt-mTOR-signaling pathway WP284
Apoptosis Modulation by HSP70 WP166
Amino Acid metabolism WP662
IL-6 signaling Pathway WP387
Statin Pathway WP1
Glutathione metabolism WP164
Blood Clotting Cascade WP460
EBV LMP1 signaling WP1243
Folic Acid Network WP1273
Triacylglyceride Synthesis WP386
Selenium Micronutrient Network WP1272
Matrix Metalloproteinases WP441
Glutathione and one carbon metabolism WP730
-log10(pval)
-log10(pval)
D
24 weeks post ACK2 versus untreated - FANCD2
Up
Down
PlurNetWork WP1763
G13 Signaling Pathway WP298
Exercise-induced Circadian Regulation WP544
TGF Beta Signaling Pathway WP113
Focal Adhesion WP85
TYROBP Causal Network WP3625
IL-5 Signaling Pathway WP151
Regulation of Actin Cytoskeleton WP523
Integrin-mediated Cell Adhesion WP6
ESC Pluripotency Pathways WP339
Focal Adhesion-PI3K-Akt-mTOR-signaling pathway WP2841
miR-127 in mesendoderm differentiation WP3991
Insulin Signaling WP65
Leptin and adiponectin WP683
Fatty acid oxidation WP2318
Alzheimers Disease WP2075
IL-2 Signaling Pathway WP450
Chemokine signaling pathway WP2292
Mitochondrial LC-Fatty Acid Beta-Oxidation WP401
Wnt Signaling Pathway and Pluripotency WP723
mRNA processing WP310
IL-5 Signaling Pathway WP151
Cytoplasmic Ribosomal Proteins WP163
EGFR1 Signaling Pathway WP572
p53 signaling WP2902
Macrophage markers WP2271
IL-6 signaling Pathway WP387
IL-3 Signaling Pathway WP373
Glutathione metabolism WP164
Folic Acid Network WP1273
Selenium Micronutrient Network WP1272
EPO Receptor Signaling WP1249
Oxidative Stress WP412
Glutathione and one carbon metabolism WP730
Toll Like Receptor signaling WP88
Glycogen Metabolism WP317
IL-1 Signaling Pathway WP37
Myometrial Relaxation and Contraction Pathways WP385
Microglia Pathogen Phagocytosis Pathway WP3626
DNA Replication WP150
-log10(pval)
-log10(pval)
E
24weeksFANCD2ACK2
24weeksFANCD2Untreated
24weeksWTACK2
24weeksWTUntreated
1weekFANCD2ACK2
1weekFANCD2Untreated
1weekWTACK2
1weekWTUntreated
Identity
Fos
Jun
Pik3r1
Akt1
Crkl
Cbl
Jak1
Jak2
Jak3
Src
Grb2
Nfl
Features
Average Expression
2
1
0
-1
Percent Expressed
25
50
75
F
ACK2 mAb
c-Kit
SOS
GRB2
SHC
JAK2
PI3K
Ras
Src
PLCy
STAT5
PDK1
MEK
Lyn/ Fyn
PKC
AKT
ERK
Proliferation Differentiation
Survival
Proliferation Migration
Proliferation
Proliferation Survival
c-Fos
c-Jun

Supplementary Figure 6: Single-Cell RNA Sequencing reveals antagonistic anti-CD117 mAb effects on MAPK pathway. (A-D) Pathway enrichment is expressed as the –log[p.value] adjusted for multiple comparisons and WikiPathways_2019_Mouse data base was used[26]. (A) Up and down regulated pathways in 1-week WT ACK2 groups compare with untreated groups. (D) Up and down regulated pathways in 1-week FANCD2-/- ACK2 groups compare with untreated groups. (C) Up and down regulated pathways in 24-weeks WT ACK2 groups compare with untreated groups. (D) Up and down regulated pathways in 24-weeks FANCD2-/- ACK2 groups compare with untreated groups. (E) Dot plot showing the average expression of selected marker genes for each group. The size of dots represents the fraction of cells expressing a given gene (>0 expression value) and the color intensity reflects the average expression level within each cluster. (F) Downregulation of MAPK pathways after c-Kit mAb inhibition.

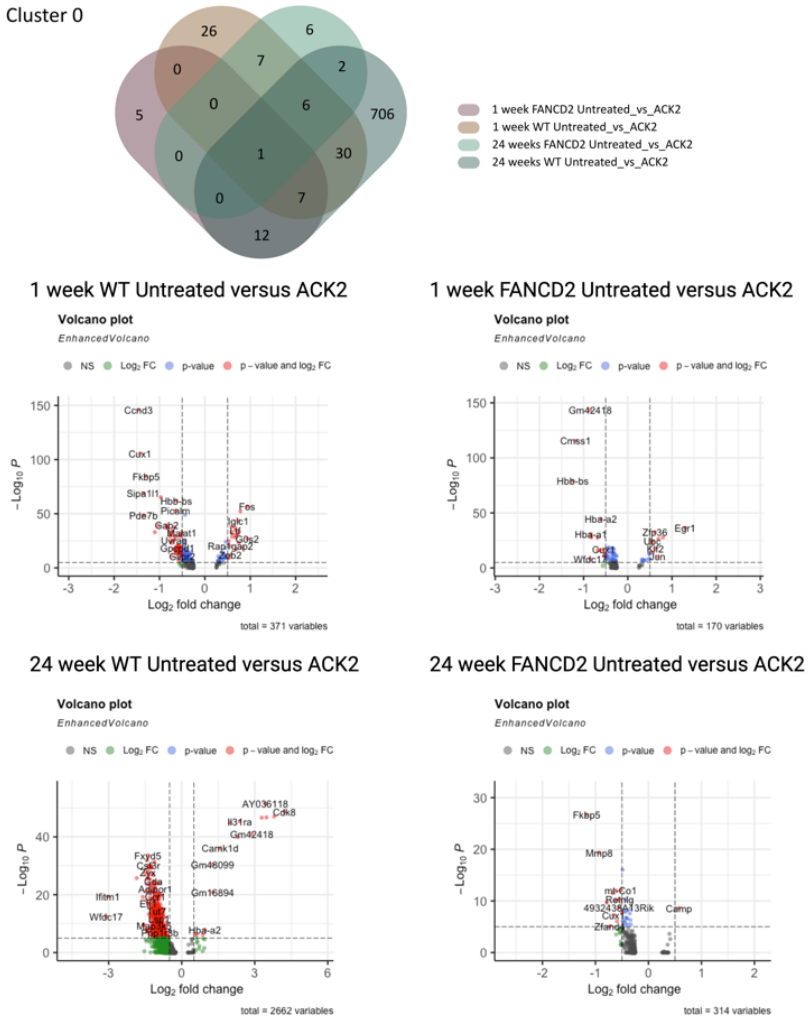

Names	Total	Elements
1 week FANCD2 Untreated_vs_ACK2 1 week WT Untreated_vs_ACK2 24 weeks FANCD2 Untreated_vs_ACK2 24 weeks WT Untreated_vs_ACK2	1	Cux1
1 week FANCD2 Untreated_vs_ACK2 1 week WT Untreated_vs_ACK2 24 weeks WT Untreated_vs_ACK2	7	Ifitm1 Il1rap Fos Hbb-bs Zfp36 Lrg1 Hba-a2
1 week WT Untreated_vs_ACK2 24 weeks FANCD2 Untreated_vs_ACK2 24 weeks WT Untreated_vs_ACK2	6	Camp Sipa1l1 Pde7b Klf13 Crispld2 Rbm47
1 week FANCD2 Untreated_vs_ACK2 24 weeks WT Untreated_vs_ACK2	12	Ier2 Nup98 Gm42418 Klf2 Wfdc17 Dennd4a Egr1 Cmss1 Il1b Ier5 Cdk8 Ubc
1 week WT Untreated_vs_ACK2 24 weeks FANCD2 Untreated_vs_ACK2	7	Mmp8 Sla Fkbp5 Nedd9 Zfand4 Ccnd3 4932438A13Rik
1 week WT Untreated_vs_ACK2 24 weeks WT Untreated_vs_ACK2	30	Antxr2 Sik3 Hectd1 Btg2 Cd33 Plin2 Sgms1 Plaur Babam2 Arl15 Ndel1 Glipr2 Dusp1 Adam19 Birc3 Picalm Arid5b Igf1r Ralgapa1 Sbno2 Tmod3 Gpcpd1 Cpne2 Tsc22d3 Fndc3b Bcl6 Gab2 Il13ra1 Ube2h Ifitm2
24 weeks FANCD2 Untreated_vs_ACK2 24 weeks WT Untreated_vs_ACK2	2	Retnlg Rdh12

Supplementary Figure 7: Differential gene expressions for each subgroup in untreated versus ACK2 treated for cluster 0 – Monocytes. (A) Venn diagram. (B) Genes in common that were up- or down-regulated across groups. (C) Volcano plot for each comparison. p-value < 0.05 and an average log2 fold change (avg_log2FC) < ±0.5.

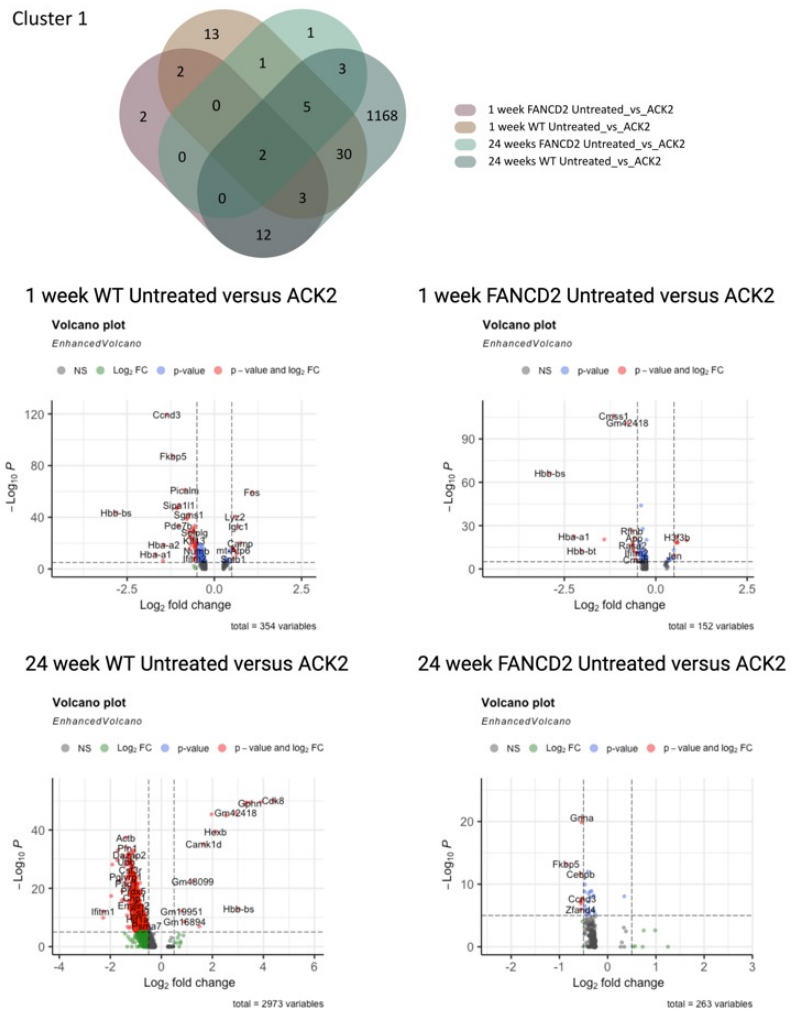

Names	Total	Elements
1 week FANCD2 Untreated_vs_ACK2 1 week WT Untreated_vs_ACK2 24 weeks FANCD2 Untreated_vs_ACK2 24 weeks WT Untreated_vs_ACK2	1	Cux1
1 week FANCD2 Untreated_vs_ACK2 1 week WT Untreated_vs_ACK2 24 weeks WT Untreated_vs_ACK2	7	Ifitm1 Il1rap Fos Hbb-bs Zfp36 Lrg1 Hba-a2
1 week WT Untreated_vs_ACK2 24 weeks FANCD2 Untreated_vs_ACK2 24 weeks WT Untreated_vs_ACK2	6	Camp Sipa1l1 Pde7b Klf13 Crispld2 Rbm47
1 week FANCD2 Untreated_vs_ACK2 24 weeks WT Untreated_vs_ACK2	12	Ier2 Nup98 Gm42418 Klf2 Wfdc17 Dennd4a Egr1 Cmss1 Il1b Ier5 Cdk8 Ubc
1 week WT Untreated_vs_ACK2 24 weeks FANCD2 Untreated_vs_ACK2	7	Mmp8 Sla Fkbp5 Nedd9 Zfand4 Ccnd3 4932438A13Rik
1 week WT Untreated_vs_ACK2 24 weeks WT Untreated_vs_ACK2	30	Antxr2 Sik3 Hectd1 Btg2 Cd33 Plin2 Sgms1 Plaur Babam2 Arl15 Ndel1 Glipr2 Dusp1 Adam19 Birc3 Picalm Arid5b Igf1r Ralgapa1 Sbno2 Tmod3 Gpcpd1 Cpne2 Tsc22d3 Fndc3b Bcl6 Gab2 Il13ra1 Ube2h Ifitm2
24 weeks FANCD2 Untreated_vs_ACK2 24 weeks WT Untreated_vs_ACK2	2	Retnlg Rdh12

Supplementary Figure 8: Differential gene expressions for each subgroup in untreated versus ACK2 treated for cluster 1 – Neutrophils. (A) Venn diagram. (B) Genes in common that were up- or down-regulated across groups. (C) Volcano plot for each comparison. p-value < 0.05 and an average log2 fold change (avg_log2FC) < ±0.5.

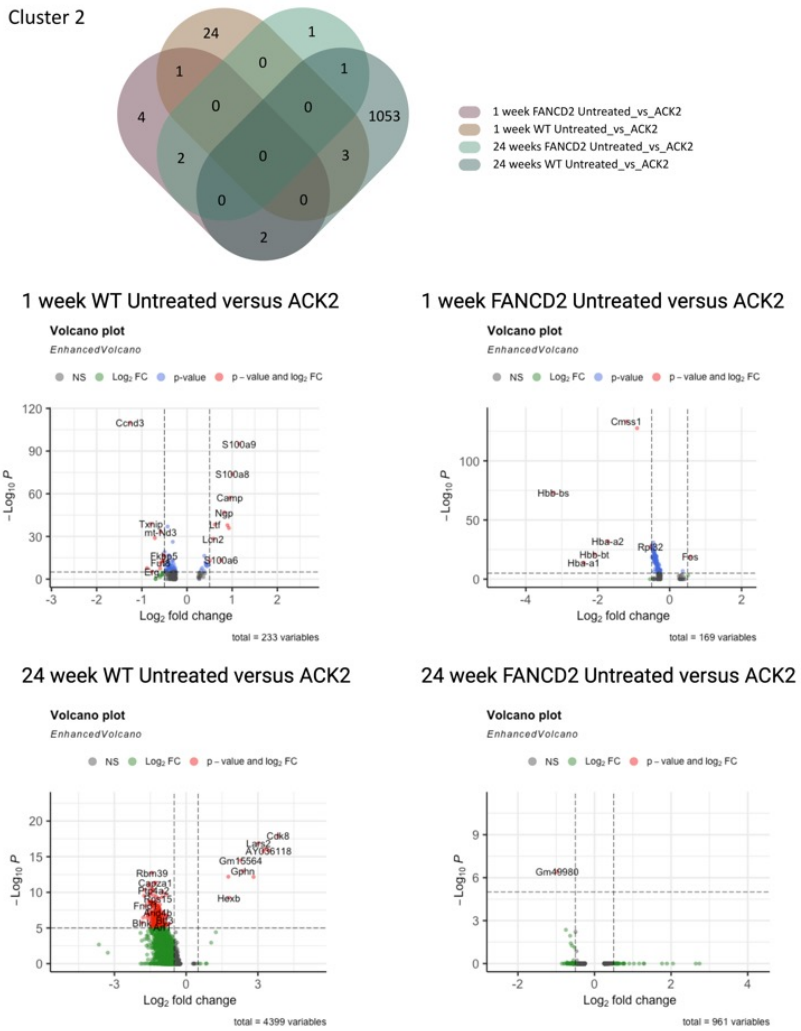

Names	Total	Elements
1 week FANCD2 Untreated_vs_ACK2 1 week WT Untreated_vs_ACK2	1	S100a6
1 week FANCD2 Untreated_vs_ACK2 24 weeks FANCD2 Untreated_vs_ACK2	2	Hbb-bs Hba-a2
1 week FANCD2 Untreated_vs_ACK2 24 weeks WT Untreated_vs_ACK2	2	Gm42418 Cmss1
1 week WT Untreated_vs_ACK2 24 weeks WT Untreated_vs_ACK2	3	S100a9 mt-Nd3 S100a8
24 weeks FANCD2 Untreated_vs_ACK2 24 weeks WT Untreated_vs_ACK2	1	Gm49980

Supplementary Figure 9: Differential gene expressions for each subgroup in untreated versus ACK2 treated for cluster 2 – B cell progenitor (A) Venn diagram. (B) Genes in common that were up- or down-regulated across groups. (C) Volcano plot for each comparison. p-value < 0.05 and an average log2 fold change (avg_log2FC) < ±0.5.

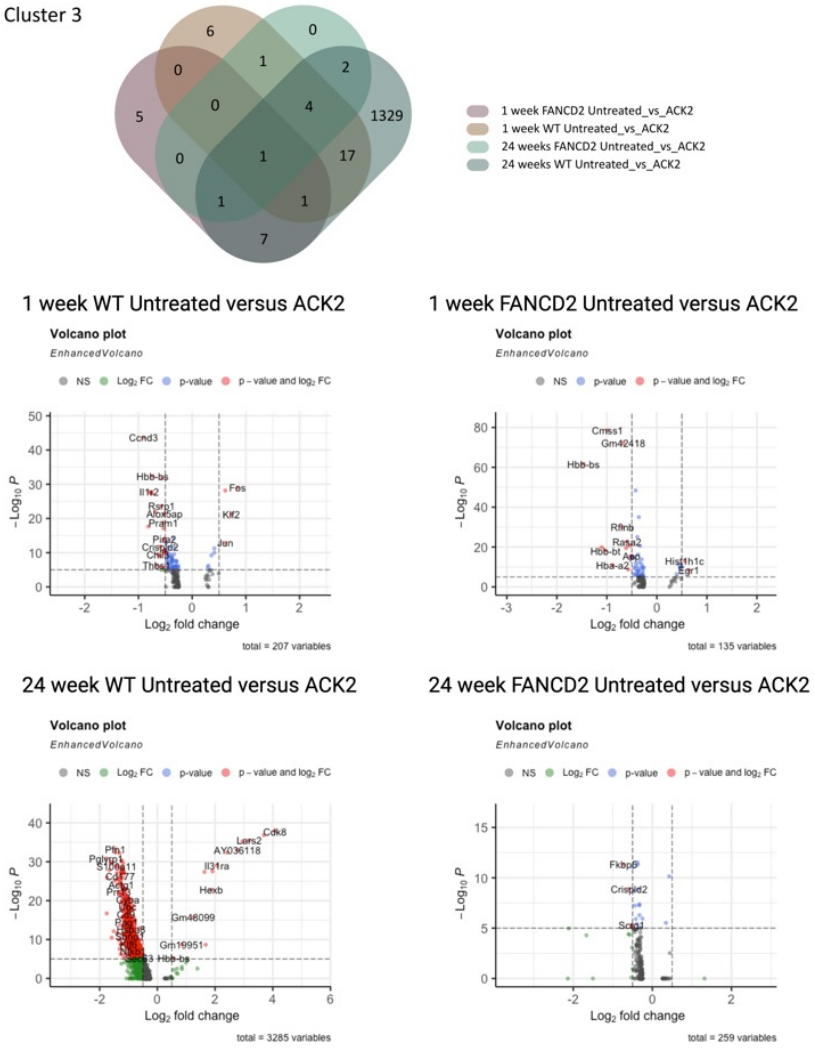

Names	Total	Elements
1 week FANCD2 Untreated_vs_ACK2 1 week WT Untreated_vs_ACK2 24 weeks FANCD2 Untreated_vs_ACK2 24 weeks WT Untreated_vs_ACK2	1	Hbb-bs
1 week FANCD2 Untreated_vs_ACK2 1 week WT Untreated_vs_ACK2 24 weeks WT Untreated_vs_ACK2	1	Ifitm6
1 week FANCD2 Untreated_vs_ACK2 24 weeks FANCD2 Untreated_vs_ACK2 24 weeks WT Untreated_vs_ACK2	1	Hba-a2
1 week WT Untreated_vs_ACK2 24 weeks FANCD2 Untreated_vs_ACK2 24 weeks WT Untreated_vs_ACK2	4	Crispld2 Cebpb Picalm Scrg1
1 week FANCD2 Untreated_vs_ACK2 24 weeks WT Untreated_vs_ACK2	7	Rasa2 Npepps App Rflnb Gm42418 Dennd4a Cmss1
1 week WT Untreated_vs_ACK2 24 weeks FANCD2 Untreated_vs_ACK2	1	Fkbp5
1 week WT Untreated_vs_ACK2 24 weeks WT Untreated_vs_ACK2	17	Sipa1l1 Klf2 Fos Thbs1 Il1r2 Clec4d Ccnd3 Pram1 Alox5ap Antxr2 Chil3 Dach1 Sgms1 Cxcr2 Hp Ccr1 Gab2
24 weeks FANCD2 Untreated_vs_ACK2 24 weeks WT Untreated_vs_ACK2	2	Zfp36l2 Retnlg

Supplementary Figure 10: Differential gene expressions for each subgroup in untreated versus ACK2 treated for cluster 3 – Monocyte/Neutrophil progenitor (A) Venn diagram. (B) Genes in common that were up- or down-regulated across groups. (C) Volcano plot for each comparison. p-value < 0.05 and an average log2 fold change (avg_log2FC) < ±0.5.

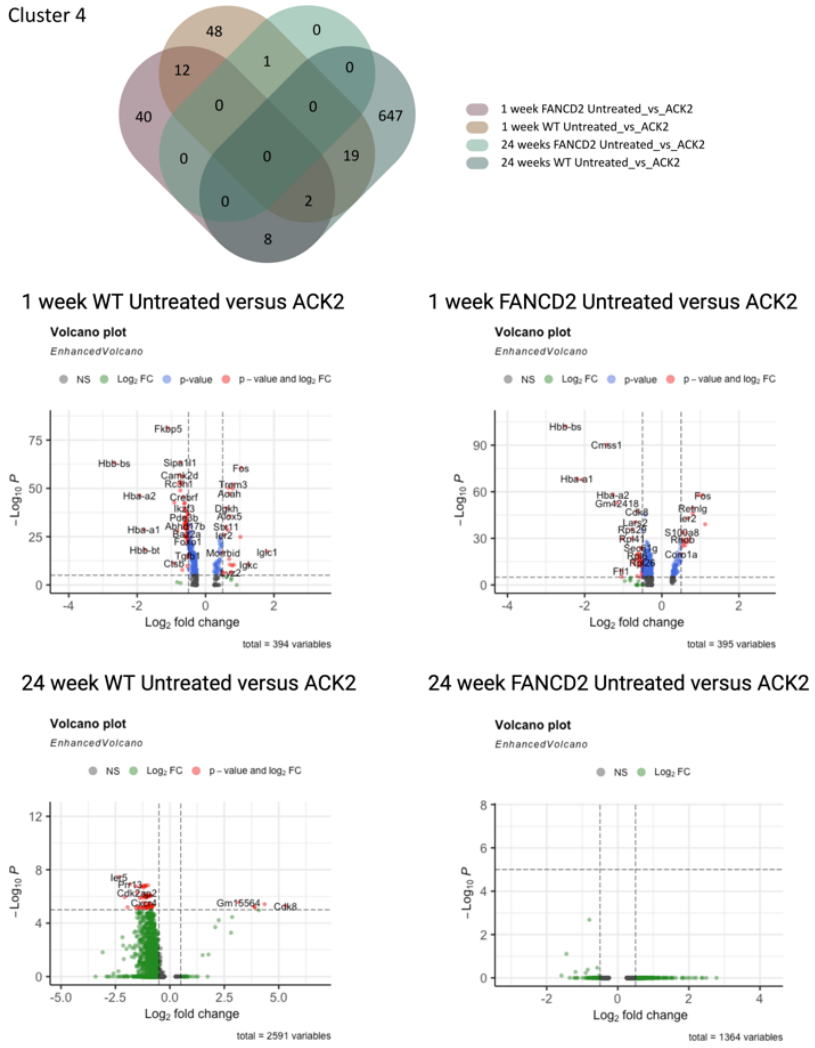

Names	Total	Elements
1 week FANCD2 Untreated_vs_ACK2 1 week WT Untreated_vs_ACK2 24 week WT Untreated_vs_ACK2	2	Gm42418 Ftl1
1 week FANCD2 Untreated_vs_ACK2 1 week WT Untreated_vs_ACK2	12	Ier2 Hba-a1 S100a8 Fos Dusp1 Hbb-bs Hbb-bt Iglc1 Igkc Hba-a2 Mmp9 Ctsb
1 week FANCD2 Untreated_vs_ACK2 24 week WT Untreated_vs_ACK2	8	Tpt1 Ccl6 Rhob Camk1d Retnlg Lars2 Cmss1 Cdk8
1 week WT Untreated_vs_ACK2 24 week FANCD2 Untreated_vs_ACK2	1	Fkbp5
1 week WT Untreated_vs_ACK2 24 week WT Untreated_vs_ACK2	19	Rassf2 Napsa mt-Atp8 Lpp Trim12a Aoah Adam19 Chil1 Padi4 Glg1 Trem3 Tgfbr2 Rbm47 Alox5 Malt1 Stx11 Cdc42se2 Dgkh Baz2a

Supplementary Figure 11: Differential gene expressions for each subgroup in untreated versus ACK2 treated for cluster 4 – Myeloid progenitor 1 (A) Venn diagram. (B) Genes in common that were up- or down-regulated across groups. (C) Volcano plot for each comparison. p-value < 0.05 and an average log2 fold change (avg_log2FC) < ±0.5.

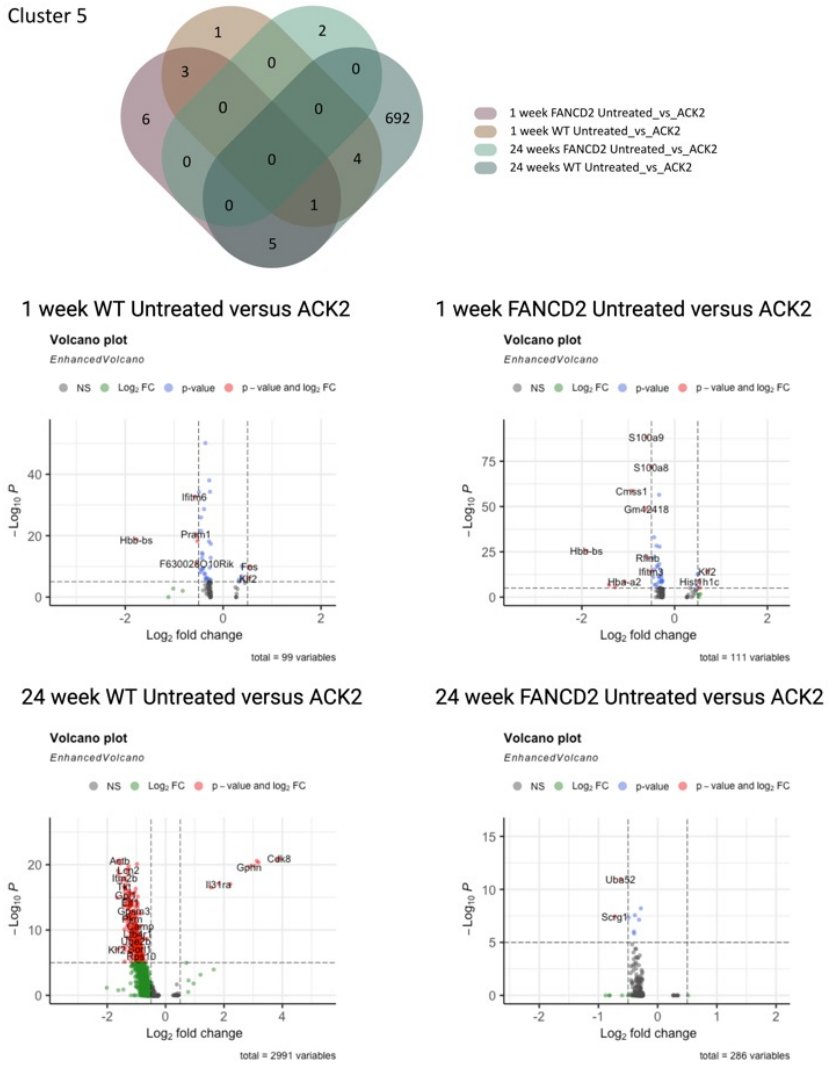

Names	Total	Elements
1 week FANCD2 Untreated_vs_ACK2 1 week WT Untreated_vs_ACK2 24 week WT Untreated_vs_ACK2	1	Klf2
1 week FANCD2 Untreated_vs_ACK2 1 week WT Untreated_vs_ACK2	3	Hbb-bs Hbb-bt Hba-a2
1 week FANCD2 Untreated_vs_ACK2 24 week WT Untreated_vs_ACK2	5	Btg2 Gm42418 Ifitm3 Cmss1 Rflnb
1 week WT Untreated_vs_ACK2 24 week WT Untreated_vs_ACK2	4	Pirb Fos Pram1 Ifitm6

Supplementary Figure 12: Differential gene expressions for each subgroup in untreated versus ACK2 treated for cluster 5 – Myeloid progenitor 2 (A) Venn diagram. (B) Genes in common that were up- or down-regulated across groups. (C) Volcano plot for each comparison. p-value < 0.05 and an average log2 fold change (avg_log2FC) < ±0.5.

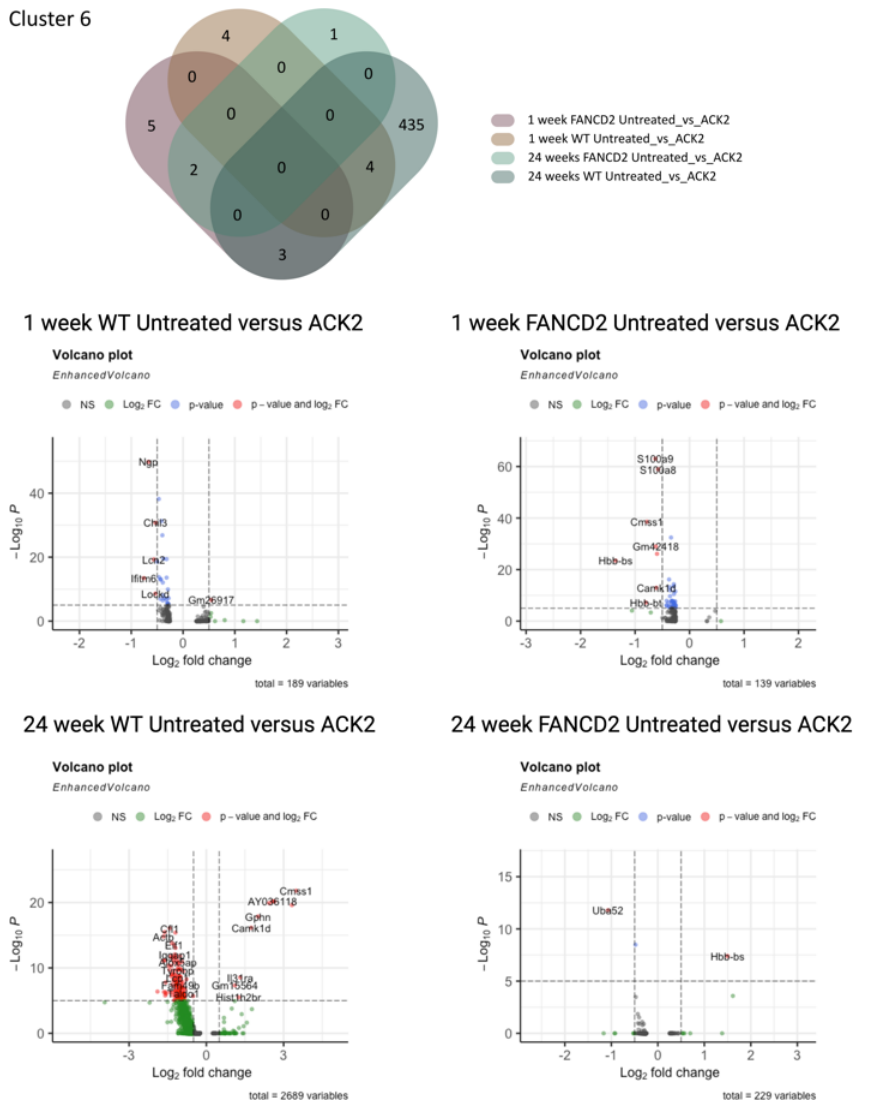

Names	Total	Elements
1 week FANCD2 Untreated_vs_ACK2 24 week FANCD2 Untreated_vs_ACK2	2	Hbb-bs Hba-a1
1 week FANCD2 Untreated_vs_ACK2 24 week WT Untreated_vs_ACK2	3	Camk1d Cmss1 Gm42418
1 week WT Untreated_vs_ACK2 24 week WT Untreated_vs_ACK2	4	Lcn2 Gm26917 Ngp Ifitm6

Supplementary Figure 13: Differential gene expressions for each subgroup in untreated versus ACK2 treated for cluster 6 – Myeloid progenitor 3 (A) Venn diagram. (B) Genes in common that were up- or down-regulated across groups. (C) Volcano plot for each comparison. p-value < 0.05 and an average log2 fold change (avg_log2FC) < ±0.5.

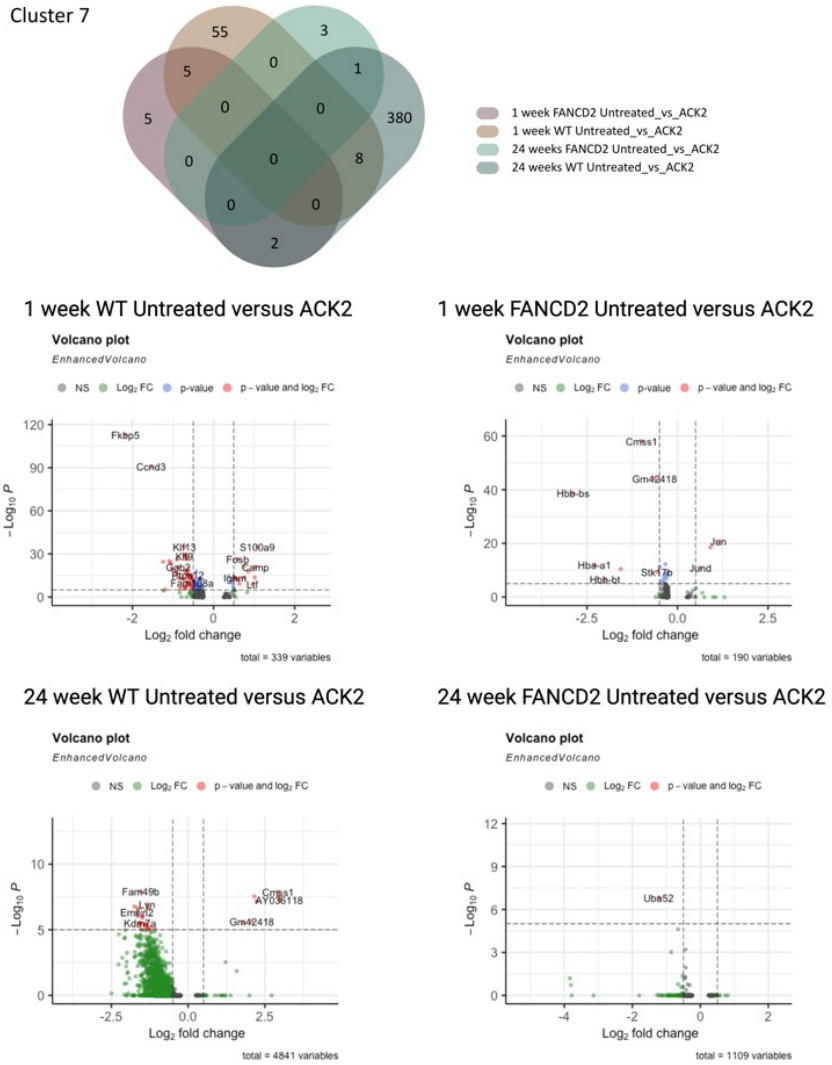

Names	Total	Elements
1 week FANCD2 Untreated_vs_ACK2 1 week WT Untreated_vs_ACK2	5	Fosb Camp Hbb-bs Hba-a2 Jun
1 week FANCD2 Untreated_vs_ACK2 24 week WT Untreated_vs_ACK2	2	Cmss1 Gm42418
1 week WT Untreated_vs_ACK2 24 week WT Untreated_vs_ACK2	8	Picalm Gsr Vcan Dock4 Stat3 Klf13 Gda Ddi2
24 week FANCD2 Untreated_vs_ACK2 24 week WT Untreated_vs_ACK2	1	Rpl5

Supplementary Figure 14: Differential gene expressions for each subgroup in untreated versus ACK2 treated for cluster 7 – Macrophages (A) Venn diagram. (B) Genes in common that were up- or down-regulated across groups. (C) Volcano plot for each comparison. p-value < 0.05 and an average log2 fold change (avg_log2FC) < ±0.5.

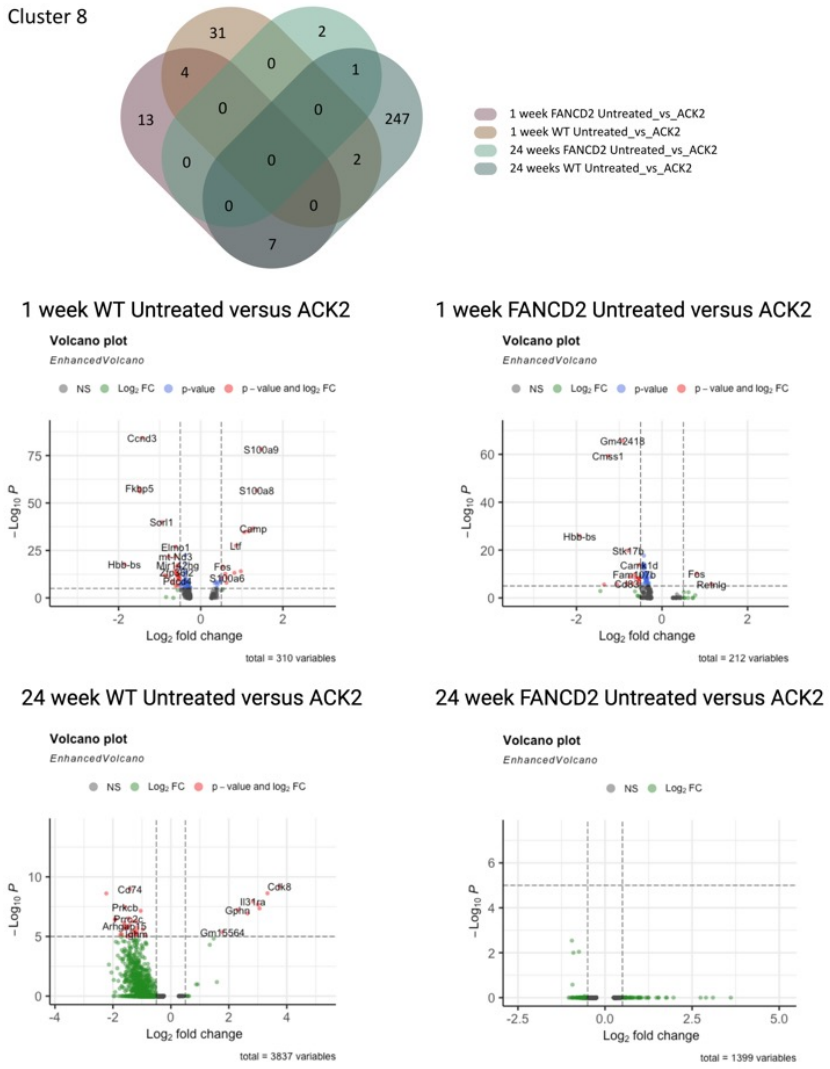

Names	Total	Elements
1 week FANCD2 Untreated_vs_ACK2 1 week WT Untreated_vs_ACK2	4	Hbb-bs Hba-a2 Retnlg Fos
1 week FANCD2 Untreated_vs_ACK2 24 week WT Untreated_vs_ACK2	7	Dennd4a Camk1d Cmss1 Gm42418 Cdk8 Fbxo11 Stk17b
1 week WT Untreated_vs_ACK2 24 week WT Untreated_vs_ACK2	4	Fchsd2 Elmo1 Foxn3 Hvcn1
24 week FANCD2 Untreated_vs_ACK2 24 week WT Untreated_vs_ACK2	1	Ebf1

Supplementary Figure 15: Differential gene expressions for each subgroup in untreated versus ACK2 treated for cluster 8 – Immature B-cell (A) Venn diagram. (B) Genes in common that were up- or down-regulated across groups. (C) Volcano plot for each comparison. p-value < 0.05 and an average log2 fold change (avg_log2FC) < ±0.5.

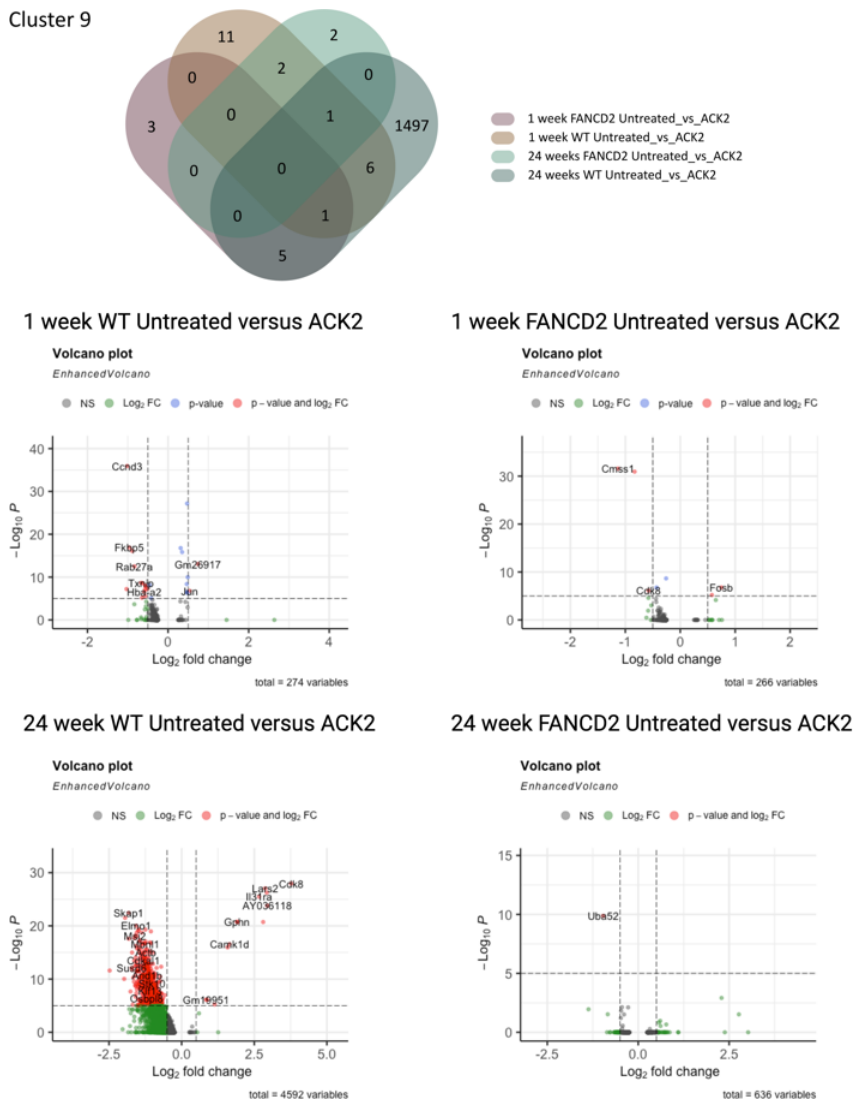

Names	Total	Elements
1 week FANCD2 Untreated_vs_ACK2 1 week WT Untreated_vs_ACK2 24 week WT Untreated_vs_ACK2	1	Jun
1 week WT Untreated_vs_ACK2 24 week FANCD2 Untreated_vs_ACK2 24 week WT Untreated_vs_ACK2	1	Hbb-bs
1 week FANCD2 Untreated_vs_ACK2 24 week WT Untreated_vs_ACK2	5	Ptpn22 Cdk8 Fosb Gm42418 Cmss1
1 week WT Untreated_vs_ACK2 24 week FANCD2 Untreated_vs_ACK2	2	Il7r Hba-a2
1 week WT Untreated_vs_ACK2 24 week WT Untreated_vs_ACK2	6	mt-Nd3 Ccnd3 Arhgap26 Serinc3 Resf1 Arhgef18

Supplementary Figure 16: Differential gene expressions for each subgroup in untreated versus ACK2 treated for cluster 9 – CLP (A) Venn diagram. (B) Genes in common that were up- or down-regulated across groups. (C) Volcano plot for each comparison. p-value < 0.05 and an average log2 fold change (avg_log2FC) < ±0.5.

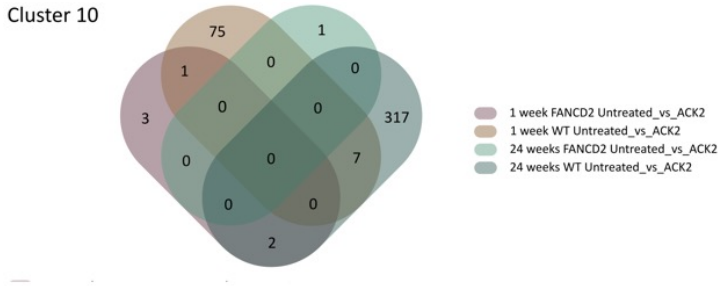

Names	Total	Elements
1 week FANCD2 Untreated_vs_ACK2 1 week WT Untreated_vs_ACK2	1	Fos
1 week FANCD2 Untreated_vs_ACK2 24 week WT Untreated_vs_ACK2	2	Cmss1 Gm42418
1 week WT Untreated_vs_ACK2 24 week WT Untreated_vs_ACK2	7	Ltf Lcn2 Camp Ngp S100a8 S100a9 Lyz2

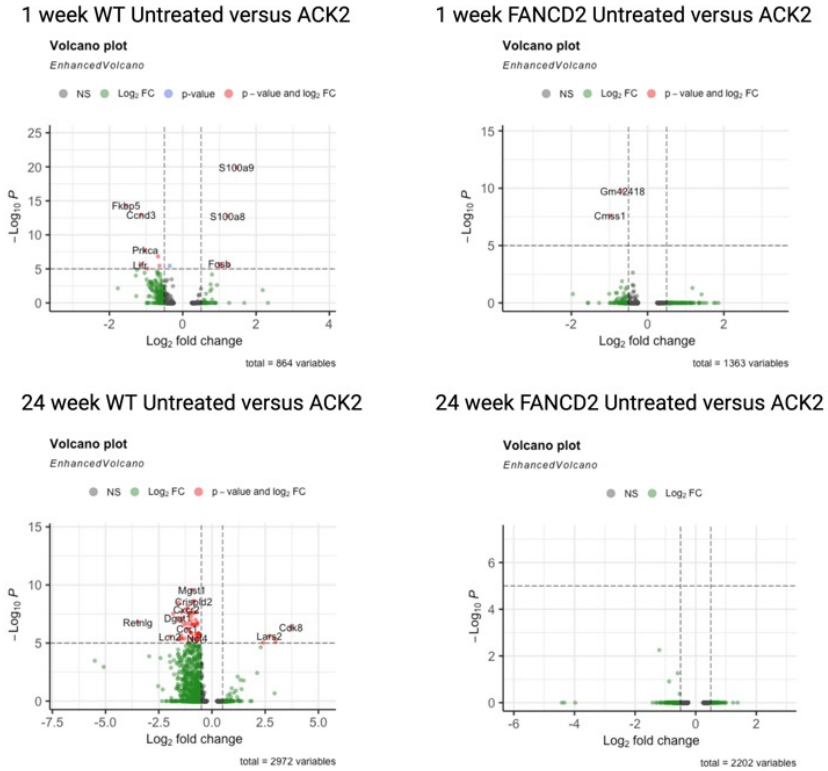

Supplementary Figure 17: Differential gene expressions for each subgroup in untreated versus ACK2 treated for cluster 10 – Dendritic cell (A) Venn diagram. (B) Genes in common that were up- or down-regulated across groups. (C) Volcano plot for each comparison. p-value < 0.05 and an average log2 fold change (avg_log2FC) < ±0.5.

Cluster 11

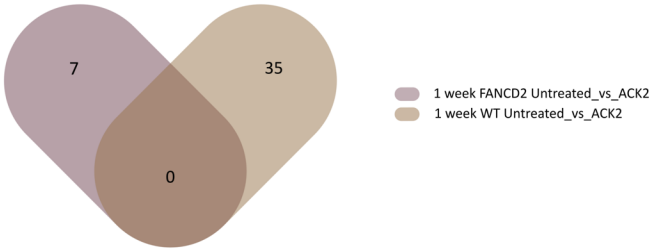

1 week WT Untreated versus ACK2

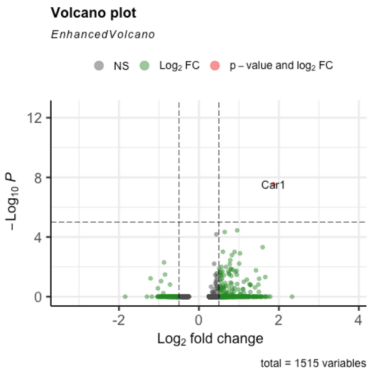

1 week FANCD2 Untreated versus ACK2

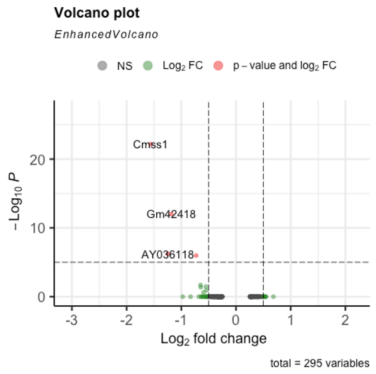

24 week WT Untreated versus ACK2

24 week FANCD2 Untreated versus ACK2

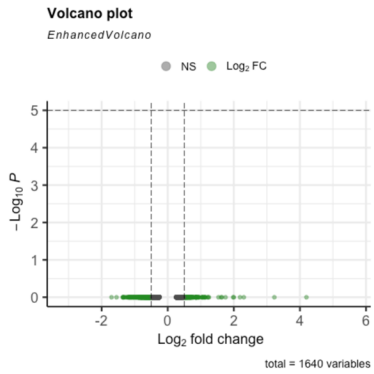

Supplementary Figure 18: Differential gene expressions for each subgroup in untreated versus ACK2 treated for cluster 11 – Erythroblast (A) Venn diagram. (B) Genes in common that were up- or down-regulated across groups. (C) Volcano plot for each comparison. p-value < 0.05 and an average log2 fold change (avg_log2FC) < ±0.5.

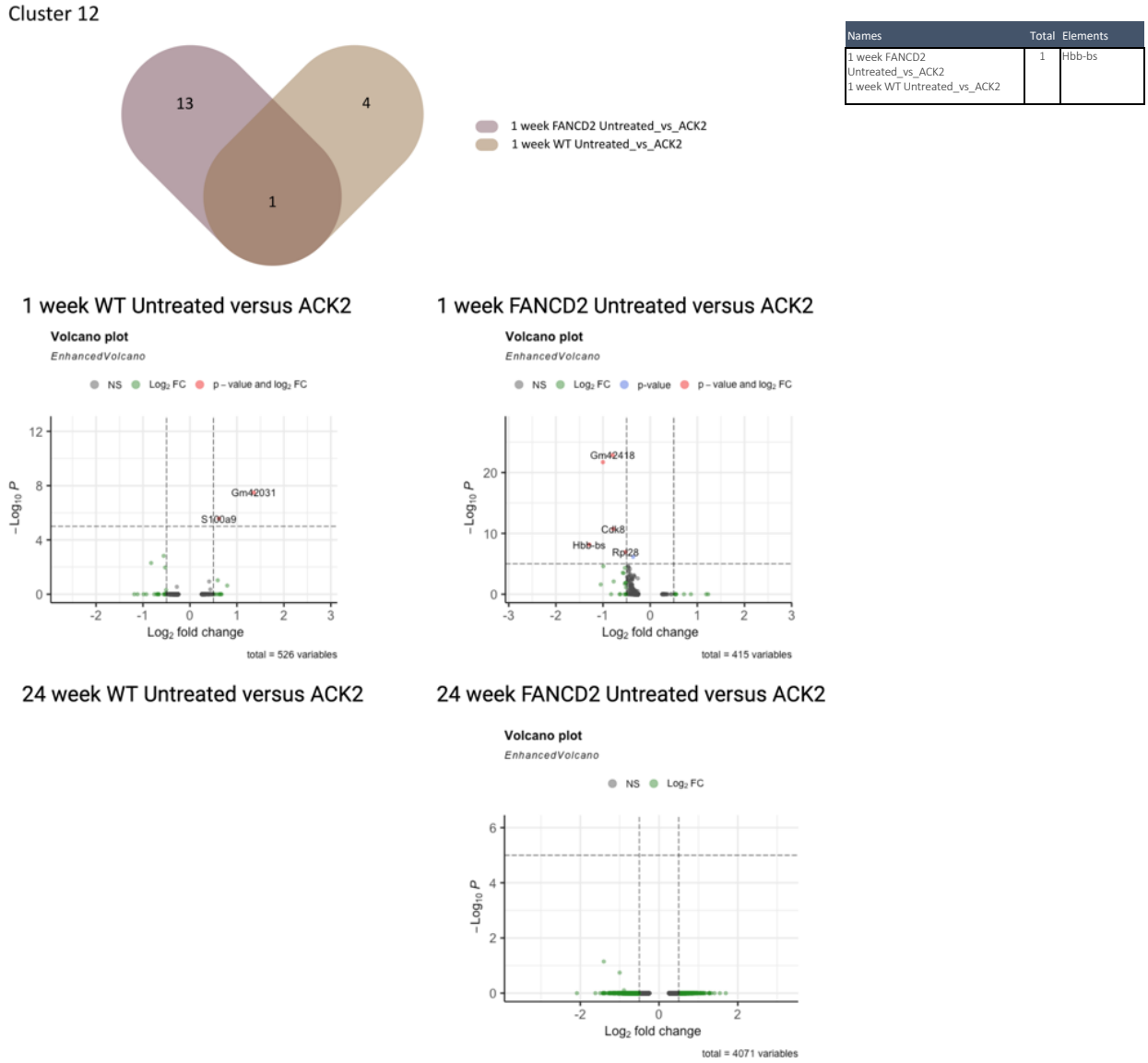

Supplementary Figure 19: Differential gene expressions for each subgroup in untreated versus ACK2 treated for cluster 12 – B cells (A) Venn diagram. (B) Genes in common that were up- or down-regulated across groups. (C) Volcano plot for each comparison. p-value < 0.05 and an average log2 fold change (avg_log2FC) < ±0.5.

Cluster 13

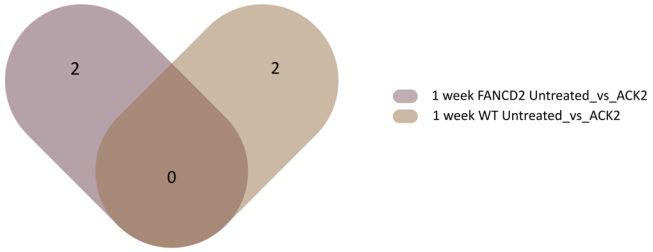

1 week WT Untreated versus ACK2

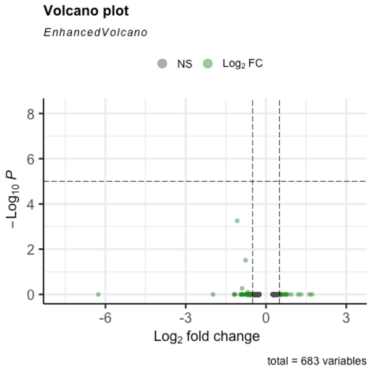

1 week FANCD2 Untreated versus ACK2

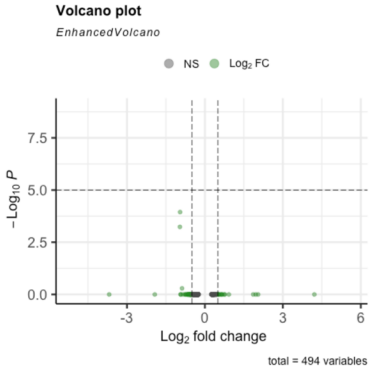

24 week WT Untreated versus ACK2

24 week FANCD2 Untreated versus ACK2

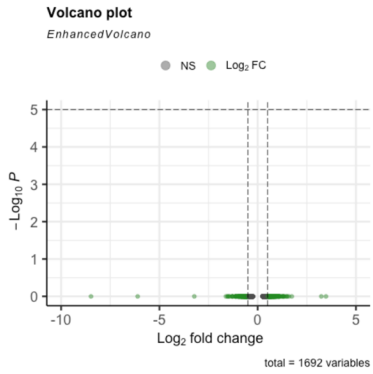

Supplementary Figure 20: Differential gene expressions for each subgroup in untreated versus ACK2 treated for cluster 13 – Plasma cells (A) Venn diagram. (B) Genes in common that were up- or down-regulated across groups. (C) Volcano plot for each comparison. p-value < 0.05 and an average log2 fold change (avg_log2FC) < ±0.5.